Influence of Solar Activity Cycles on Earth's Climate

Executive Summary Report

Freddy Christiansen, Danish National Space Center
Joanna D. Haigh, Imperial College
Henrik Lundstedt, Swedish Institute of Space Physics

ESTEC Contract no. 18453/04/NL/AR
Issue 1, September 5, 2007

ESA STUDY CONTRACT REPORT - SPECIMEN

No ESA Study Contract Report will be accepted unless this sheet is inserted at the beginning of each volume of the Report.

ESA CONTRACT No 18453/04/NL/AR	***SUBJECT*** Influence of Solar Activity Cycles on Earth's Climate		**CONTRACTOR** Danish National Space Center
*** ESA CR( )No 18453**	*** STAR CODE**	**No of volumes 1** **This is Volume No 1**	**CONTRACTOR'S REFERENCE DNSC_ISAC_Sum Rep**

ABSTRACT:
This Executive Summary Report presents the most important results found during the ISAC (Influence of Solar Activity Cycles on Earth's Climate) study. The study group, involving researchers from Danish National Space Center, Imperial College, and Swedish Institute for Space Physics, has investigated the coupling between solar and climate variations. A comprehensive data base of solar observations has been compiled and correlations between the various solar parameters were investigated using both ordinary correlations analysis as well as wavelet analysis. Based on physical theories of solar influences in the climate a few parameters of the multitude of solar observations were selected for correlation analysis with climate observations. Together with internal climate parameters, such as the NAO, QBO, ENSO, and volcanic aerosol indices, the solar parameters were used in multi-regression and correlation analyses with a selection of climate parameters focusing mainly on temperatures, cloud cover, and winds, but also giving examples for other parameters. Furthermore, a review of the most important solar-climate interaction mechanisms and climate modelling were presented.

The work described in this report was done under ESA Contract. Responsibility for the contents resides in the author or organisation that prepared it.

Names of authors: Freddy Christiansen, Joanna D. Haigh, and Henrik Lundstedt

**** NAME OF ESA STUDY MANAGER Chung-Chi Lin** **DIV: Instrument Pre-development (EOP-PIM)** **DIRECTORATE: Earth Observation Programmes**	**** ESA BUDGET HEADING G/1/100.060/600.5100/GE+/RD100/04S10**

Preface

This Executive Summary Report highlights the most important results obtained during the ISAC (Influence of Solar Activity Cycles on Earth's Climate) study. During the ISAC study the following task were carried out:

1) Literary Survey on Sun-Earth Connection
2) Identification of Relevant Data
3) Data Interpretation
4) Quantification of Global Climate Modulations
5) Hypothetical Mechanisms
6) Investigation of Modelling Potentials
7) Conclusions and Recommendations

A thorough summary is presented in the Task 7 Final Report (DNSC Scientific Report 2/2007), here we focus on a few main points together with the conclusions and recommendations.

The ISAC study has been carried out by groups at the Danish National Space Center (now part of the Danish Technical University), Copenhagen, Denmark, the Swedish Institute of Space Physics (IRF), Lund, Sweden, and the Space and Atmospheric Physics Department, Imperial College, London, UK. Apart from the authors listed for this report the following have contributed to the ISAC study and therefore also to this summary: Nigel D. Marsh, Torsten Bondo, and Henrik Svensmark, DNSC, Peter Wintoft and Fredrik Boberg, IRF, and Wenya Zhong and Isla Simpson, IC.

Abstract

This Executive Summary Report highlights the most important results found during the ISAC (Influence of Solar Activity Cycles on Earth's Climate) study. The study group, involving researchers from the Danish National Space Center, Imperial College, and the Swedish Institute for Space Physics, has investigated the coupling between solar and climate variations. A comprehensive data base of solar observations has been compiled[1] and correlations between the various solar parameters were investigated using both ordinary correlations analysis as well as wavelet analysis. The wavelet analysis supplements the ordinary correlation analysis by providing a more detailed look into temporal changes in the interdependence of solar output parameters. Based on current physical theories of solar influences on the climate a few parameters of the multitude of solar observations were selected for correlation analysis with climate observations, mainly total solar irradiance (TSI), ultra-violet radiation (UV), and galactic cosmic rays (GCR), but also the solar wind (SW) and precipitating particles (HPI) were studied. Together with internal climate parameters, such as the NAO, QBO, ENSO, and volcanic aerosol indices, the solar parameters were used in multi-regression and correlation analyses with a selection of climate parameters focusing mainly on temperatures and cloud cover. Studies of other parameters are presented in the final report and in the individual task reports.

We focus here on the most prominent results obtained in the correlation study of solar variability and climate responses in the stratosphere and troposphere and give only a cursory review on the subjects of surface response and solar-climate interaction mechanisms and modelling. The summary of each section does, however, refer to the results not presented here. The interested reader is referred to the individual reports and the Final Report (DNSC Scientific Report 2/2007).

1 Introduction

Never before has the state of Earth's climate been so much in the public's eye. Global warming is a major concern of the world with its potentially devastating effects on coastal areas and agricultural production. The steep rise in greenhouse gas emissions since the start of the industrial era has increased the CO_2 concentrations in the atmosphere by 30%. This is widely believed to be the dominant cause of the observed rise of about 0.6^{o}C in the global mean surface temperature during this period. A small systematic rise or fall in the global temperature is caused by a net imbalance in the Earth's radiation budget. The present net radiative forcing from manmade constituents (greenhouse gases and aerosols) is estimated to be about 1.2 Wm^{-2}. The climate models upon which the predictions of greenhouse warming depend provide a reasonable representation of the observed variations in global temperature over the last century. However, they remain subject to significant uncertainties, especially from feedback mechanisms and from the effects of anthropogenic aerosols.

In order to determine the influence of mankind on climate change it is important to understand the natural causes of climate variability. A natural effect that has been hard to understand physically is an apparent link between climate and solar activity. From

[1] The data base is hosted by the Swedish Institute of Space Physics and is available through Henrik Lundstedt (Henrik@lund.irf.se).

historical and geological records there are strong indications that the sun has played an important role in the past climate of the Earth, but the physical mechanism is currently unknown. Whatever mechanism caused those earlier changes would most likely also be operating today and may have been active throughout the history of our planet. There have been several attempts to explain the link between solar activity and climate from variations in the sun's radiative output. These have tended to rely on simulations involving Global Climate Models (GCM), which are limited by our current understanding of the fundamental physics. The aim of this study has been to enhance this understanding and point to areas where further research and observations are needed.

The variable Sun

Solar activity varies on time-scales from hours to billions of years. One aspect of this variability is related to solar magnetic fields generated below the convective zone in the interior. The evolution of magnetic fields results in many manifestations, on time-scales in the range of hours to several hundred even thousand years, such as the well-known sunspot cycle and its longer-period modulations, solar wind structures, and coronal mass ejections.

A number of mechanisms by which the Sun can influence Earth and the climate have been suggested. The influences from the variation of the electromagnetic radiation are most often considered. However, a changing solar wind and energetic particles can also influence Earth either directly or indirectly through modulating the cosmic ray flux. Several of these mechanisms may influence Earth simultaneously. With this very complex scenario it is not a surprise we detect many solar signals in climate records.

Different kinds of indicators for solar activity have been used in the literature. The most well known and most often used is the sunspot number that has been recorded since the early 17th century (Figure 1). The 11-year sunspot cycle (Schwabe, 1844) is also the most well known solar variability. This cycle results from active region migration, evolution, submerging, and annihilation. Although the period is 11 years on average, this sunspot cycle is varying in both length and amplitude. As a result of this cycle, the global solar magnetic polarity is reversed approximately every 11 years, giving a total solar magnetic cycle period of 22 years. Modulating the 11-year sunspot cycle is the Gleissberg cycle with a period around 88 years. The Gleissberg cycle has been detected in sunspot data (Frick et al., 1997; Ogurtsov et al., 2002), solar cosmic ray activity (McCracken et al., 2001), and in solar energetic particle events (Reames, 2004). By using cosmogenic isotopes it has been shown that the Gleissberg cycle is valid for extended time spans (Peristykh and Damon, 2003; Usoskin et al., 2004). Solar cycles with even longer periods have been proposed, such as the 205-year de Vries cycle (Beer, 2000; Wagner et al., 2001) and the 2,100-year Hallstatt cycle (Damon and Jirikowic, 1992).

Changes in sunspot number are manifestations of the dynamics of the internal dynamics of the Sun and are accompanied by changes in virtually every other output from the Sun such as the radiated energy in the form of the Total Solar Irradiance as well as in every part of the radiated spectrum (X-rays, gamma-rays, UV, or radio flux), particle streams from the Sun (solar wind, coronal mass ejections, solar energetic particles, or solar flares) and also influences solar modulated parameters such as galactic cosmic rays and cosmogenic isotopes; Figure 2 displays a few of these. This simultaneous variation of basically all solar and solar-modulated parameters is a significant problem when aiming

to pin-point a single solar source to an observed climate variation, since the observed changes in various climate parameters correlate equally well with more than one solar-related index.

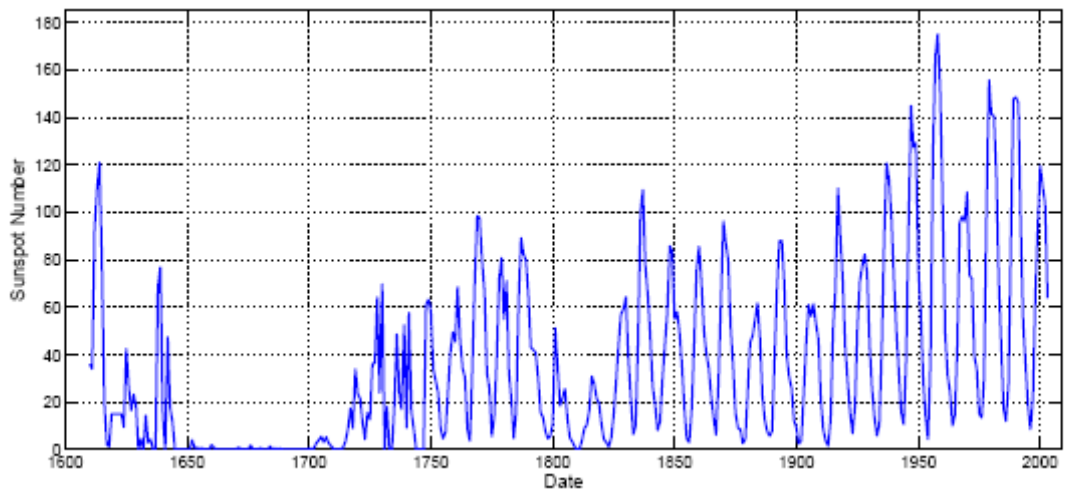

Figure 1: Smoothed yearly sunspot number for the period 1610 to 2003. The clear 11-year sunspot cycle is modulated with an 88-year Gleissberg cycle with the distinct Maunder Minimum (1645-1715) with almost no visible sunspots.

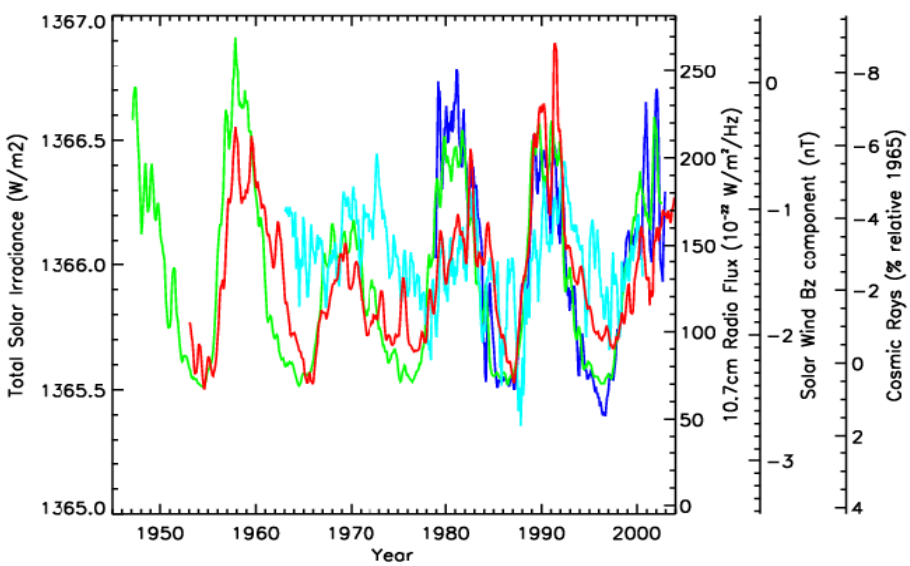

Figure 2: Monthly observations of TSI (blue) together with other solar parameters influencing Earth's environment: 10.7cm Radio Flux often used as a proxy for Solar UV (green), Solar Wind Bz component (light blue), and Cosmic Rays (red). All data have been smoothed with a 5-month running window.

The Sun-climate connection

The observation that warm weather seems to coincide with high sunspot counts and cool weather with low sunspot counts was made as long ago as two hundred years by the astronomer William Herschel (Herschel, 1801; Hoyt and Schatten, 1992). Herschel noticed that the price of wheat in England was lower when there were many sunspots,

and higher when there were few. Since the time of Herschel there have been numerous observations and non-observations of an apparent link between climate and the sunspot cycle, a large number of these have previously been recorded in various review articles and books on the subject (e.g., Dickinson, 1975; Herman and Goldberg, 1978; Hoyt and Schatten, 1997).

It is often global temperature that is used as the key parameter for demonstrating variability in the average state of Earth's climate. One example of a positive correlation is the apparent solar response of Sea Surface Temperatures (Reid, 1987; Reid, 1991; Reid, 2000). Sea Surface Temperatures (SSTs) have been obtained from ocean going ships since the middle of the 19th century. During the first part of the 20th century the observed SSTs increased, and then flattened out during the years 1940 and 1970, before continuing with the overall increasing trend. Figure 3 indicates that this long-term variability in SSTs is in phase with the 80-90 year envelope that modulates the approximately 11-year sunspot cycle.

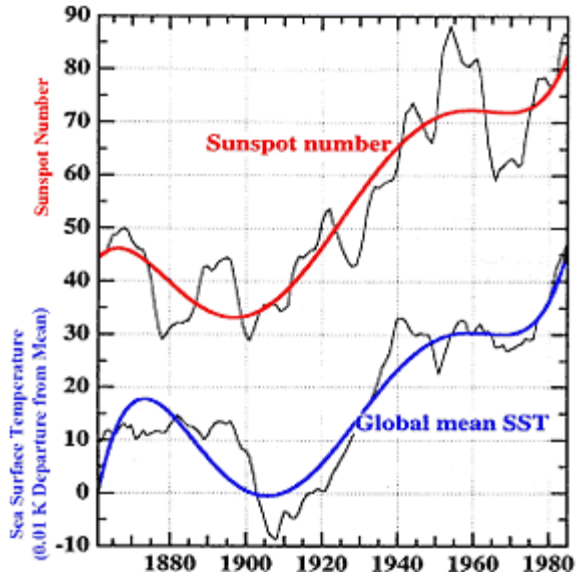

Figure 3: 11 year running mean of the annual sunspot numbers (upper thin curve), and the mean global sea-surface temperature anomaly (lower thin curve). The heavy curves represent a 7th degree polynomial least squares fit to the data. Units for the lower curves are 0.01K departures from the 1951-1980 average.

White et al (1997) confirmed this finding with two independent SST datasets, i.e., surface marine weather observations (1900-1991) and upper-ocean bathythermograph temperature profiles (1955-1994). The highest correlations were obtained with ocean temperatures lagging solar activity by 1-2 years, which is roughly the time scale expected for the upper layers of the ocean (<100m) to reach radiative balance following a perturbation in TSI. From simple energy balance arguments White et al (1997) estimated climate sensitivities due to changes in TSI at the ocean surface to be 0.2-0.4^{o} K/(Wm^{-2}). This suggests that a 0.04-0.09^{o} K change in SSTs would be expected from a 1 Wm^{-2} change in TSI at the top of the atmosphere. While these estimates are of a similar order of magnitude to the observed changes in global SSTs, they are on the low side, suggesting a possible amplification of the solar signal exists within the climate system.

Radiosonde observations of tropospheric temperatures over the period 1958 - 2001 display significant variability at a number of different time-scales. From monthly data the effects of El Nino and volcanic eruptions are particularly evident. However, these features are largely removed when filtering with a three-year running mean, and the low pass Tropospheric temperatures show a remarkably good agreement with changes in reconstructed Total Solar Irradiance (TSI). Figure 4 indicates that an increase in reconstructed TSI of 1 Wm^{-2} coincides with an increase of ~0.4^o K in tropospheric temperatures. An expected temperature response from the reconstructed changes in TSI can be estimated with a simple climate sensitivity analysis. Assuming a climate sensitivity of 0.6-0.8^o K/(Wm^{-2}), estimated from the average response of climate models to a doubling of CO_2 (e.g., Appendix 9.1 - Houghton et al., 2001), predicts that a 1 Wm^{-2} change in TSI at the top of the atmosphere would result in only ~0.1^{o}K change in temperature. Clearly, changes in TSI alone are too small to explain the observed Tropospheric temperature variability and an amplification factor is required (Marsh and Svensmark, 2003b).

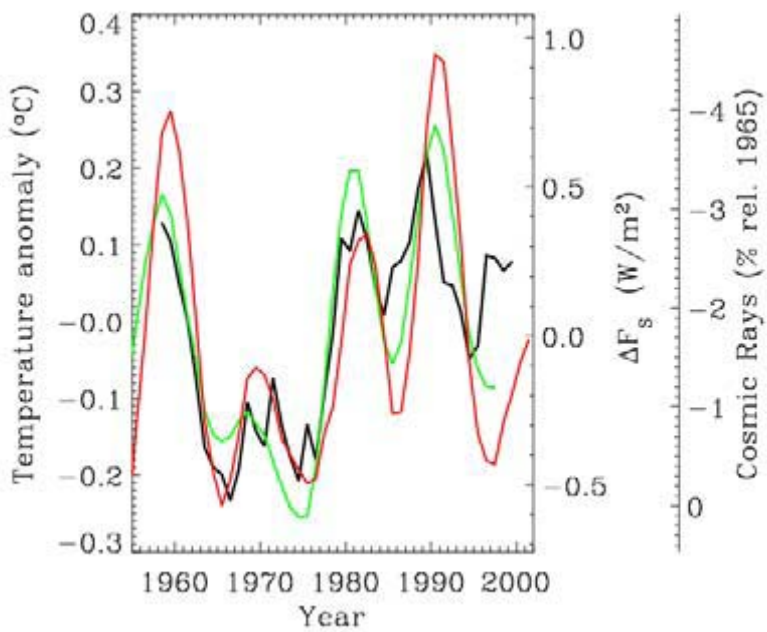

Figure 4: Tropospheric temperatures (black), obtained from radiosondes, shown together with reconstructed TSI (green), ΔF_s, using re-scaled sunspot numbers as a proxy and cosmic rays (red). Both data sets have been low pass filtered with a three year running mean (adapted from Marsh and Svensmark, 2003b).

2 Solar Activity

The solar magnetic activity often shows non-linear, transient and chaotic behavior. For that reason wavelet analysis methods are employed in order to compare the indicators with the mathematical concepts, such as the toroidal and poloidal magnetic fields. Wavelet analysis is a powerful tool both to find the dominant mode of variation and also to study how it varies with time, by decomposing a non-linear time series into time-frequency space. For details of the wavelet methods used here, see Liszka (2003), Lundstedt et al. (2005), and Lundstedt et al. (2006).

In Figure 5 the solar activity, as indicated by the group sunspot number and sunspot number, is given in an ampligram for the period 1610 to 2005. The variability is shown for fractions of the maximum wavelet coefficient magnitude. The large variation of the solar activity amplitude is clearly seen, including several minima such as Maunder minimum (1645-1715), Dalton minimum (1795-1823), and the most recent maximum (after 1940). The sunspot indicator shows the 11 year cyclicity for the whole period except during the Maunder minimum. In the lower panel only the weak signal, below 20%, of the WCM maximum is shown. It is interesting that even the very weak signal has structures.

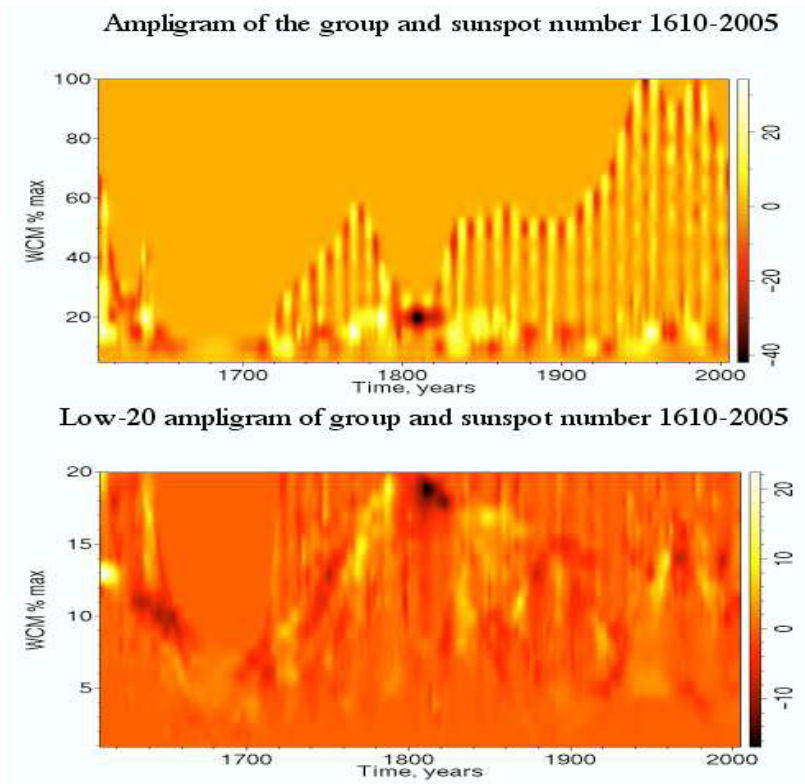

Figure 5: Ampligram of the group sunspot number 1610-1995 and the sunspot number 1995-2005. In the lower panel only the weak signal, below 20 % of WCM maximum. In the colour scale to the right, the zero represents the average value of the sunspot number.

In order to further study the cyclicity, revealing maximum and minimum, during the Maunder Minimum we carried out a Multi-Resolution Analysis of the annual ^{14}C production rate (Figure 6). The variation is studied at different resolutions. At level four in the detailed part the 22-year cycle is clearly present during the Maunder Minimum. The 11-year cycle is also clearly seen at level three in the detailed part. At the lowest resolution (approximation level four) several peaks appear. The strongest occur around 1600 and about 1780. These are not seen in the group sunspot number. The found cyclicity for the solar indicator, ^{14}C production rate, during the Maunder minimum shows that this indicator is better than the sunspot number. The explanation for the difference is that during the Maunder minimum strong toroidal magnetic flux tubes (as indicated by the sunspot number) were absent but weak ephemeral magnetic fields (also indicated by the ^{14}C production rate) were present.

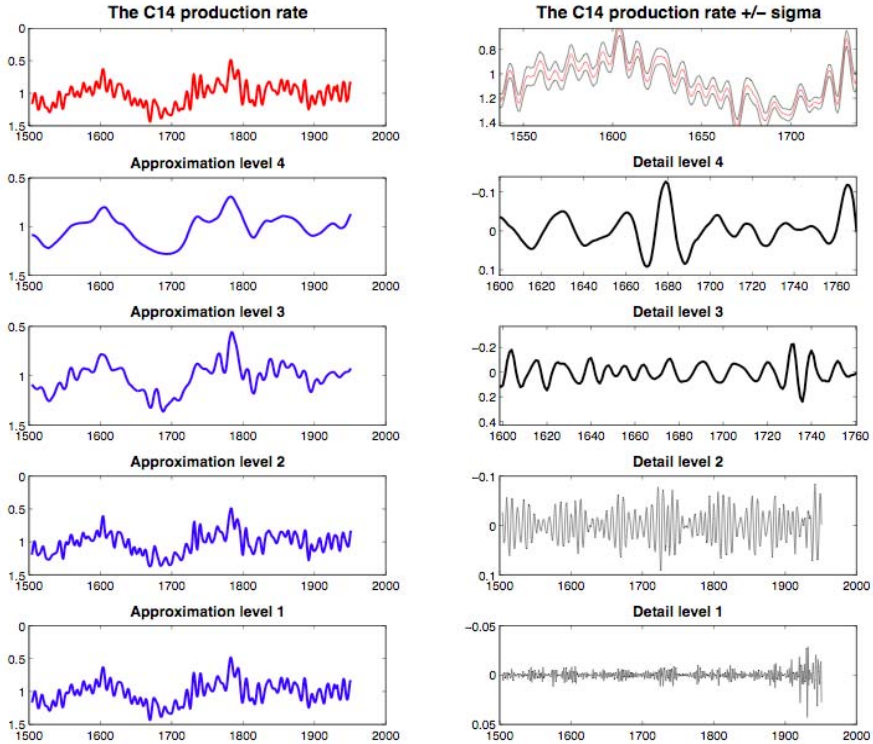

Figure 6: Multi resolution analysis of the ^{14}C production rate. The 22-year cycle is clearly present during the Maunder minimum (zoomed in period) at detail level 4. The 11-year cycle is clearly present during the Maunder Minimum (zoomed in period) at detail level 3.

During the latest solar cycle, the sunspot number has again shown to be a not so good indicator of the solar activity. On September 7, 2005, an X17 solar flare occurred and we have had as many geomagnetic storms and X-type solar flares in 2005 (i.e. close to sunspot minimum), as during Solar Max (2000). To improve the picture of the Sun's activity we need an indicator describing the activity of the whole Sun from below the solar surface, on the surface to the corona. Using the sunspot number we only describe the activity of largest flux tubes on the surface below about 35 degrees latitude.

For the use in climate analysis it is interesting to compare the most often used parameters such as sunspot number (Rz), solar irradiance (TSI), cosmic rays (CLIMAX), and UV. Figure 7 shows the wavelet coherence between Rz and TSI. In the top panel the wavelet coherence is shown and for comparison Rz is shown in the bottom panel. For periods longer than 64 Carrington rotations (about 5 years) there is a significant correlation with no phase difference (right pointing arrows). At one year period (Period=13) the correlation is more patchy, and when there is a correlation the signals are basically out of phase and that the correlation mainly exists during the declining and minimum phases of Rz. It is clear that if Rz is used as a proxy for TSI care has to be taken to which process should be modelled if any temporal averaging is used. If we study periods in the range 8 days to 1.4 years there is a quite strong negative correlation which could be related to the sunspot blocking. For periods longer than 2.8 years, or even 5.6 years, the correlation is strongly positive probably due to the fact that bright regions and sunspots correlate on these time scales.

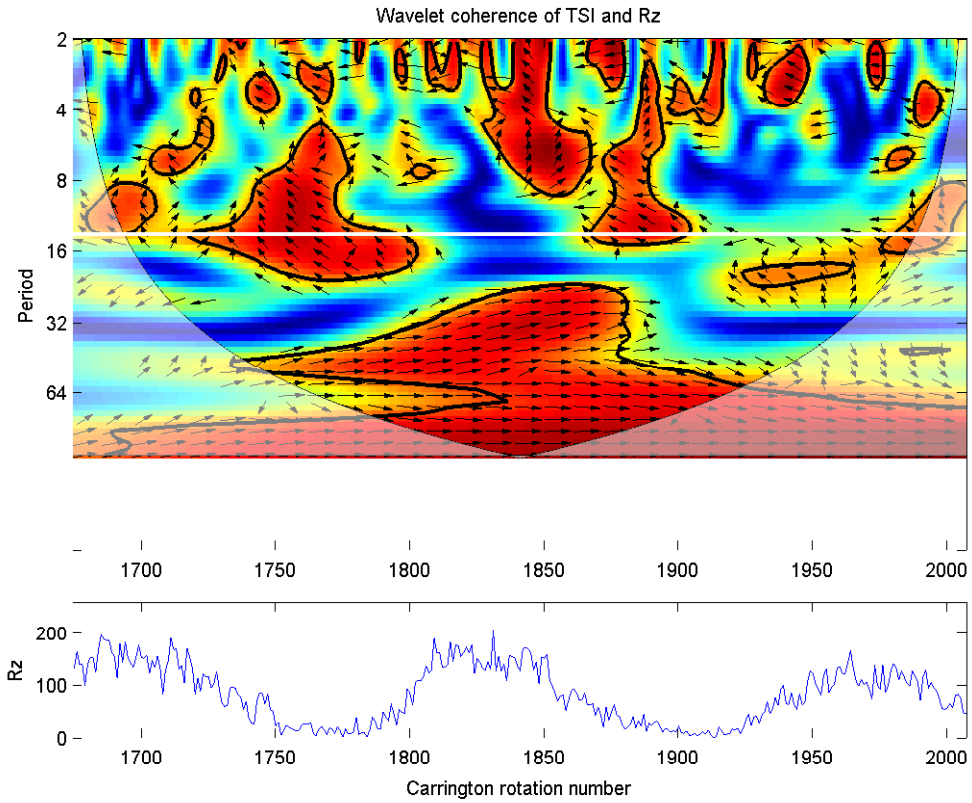

Figure 7: Wavelet coherence between TSI and Rz. Upper panel: Weak correlation is coloured blue and strong correlation red. The black heavy lines indicate a significant correlation at the 95% level. Arrows indicates any phase shift. An arrow pointing to the right means no phase shift, an arrow pointing down means that TSI leads Rz by 90 degrees, an arrow pointing up means that TSI lags Rz by 90 degrees, and an arrow pointing to the left means that they are 180 degrees out of phase. The period is given in units of Carrington rotations. The thick white line marks 1 year periodicity. Lower panel: The sunspot number Rz is shown for comparison.

A similar analysis for sunspot number and cosmic rays shows that significant and strong anti-correlation is present at all times for periods longer than about 100 Carrington rotations (7 years) but for shorter periods the signals only occasionally correlate. Thus, on long time scales Rz may serve as a good proxy for the cosmic ray flux, but not on shorter time scales.

When solar activity is discussed it is insufficient to speak in terms of sunspot numbers and 11-year cycles as there is wide range of processes taking place on different time scales. The prime cause of all solar variability is the changing solar magnet field. For example, sunspots are caused by strong magnetic flux penetrating the photosphere and thereby suppressing outgoing radiation leading to a lowering of TSI. However, sunspots appears in active regions where also bright features like plages appear giving a positive contribution to the TSI. On larger scales there is also a network of fields giving increased brightness with a positive contributing to the TSI. This complex response of the TSI to magnetic fields is partly seen in the TSI–Rz correlation in Figure 7. A similar correlation is seen between the F10.7 cm radio flux and TSI. Thus, any solar–climate study that uses Rz or F10.7 as a proxy for TSI must be carefully thought through. If monthly averages

are used there will be a mixture of processes working on different temporal scales that will have opposite effects on TSI. We therefore suggest that a scale based approach should be used when Rz or F10.7 is used as a proxy for TSI so that the solar–climate relation is studied on a scale-by-scale basis. Rz and cosmic rays shows a simpler relation in the sense that they are anti-correlated on all scales, although the correlation is very weak for temporal variations shorter than 2.8 years. The weak correlation on time scales shorter than 2.8 years are only occasional covariation. A similar conclusion is reached if F10.7 is used. Thus, if Rz or F10.7 is used as a proxy for the cosmic ray flux one can only expect to find a strong Sun–climate correlation at time scales of several years and longer. A weak, or lack of, Sun–climate correlation on time scales from months to about 2–3 years using Rz as a proxy for cosmic rays can not be used to rule out a relation.

3 Stratospheric Interactions

We focus in what follows on deriving the solar signal in stratospheric temperatures and zonal winds. To this end we apply a multiple regression technique to zonal mean data from the NCEP/NCAR reanalysis data set. Because our work, as previous studies, suggests that the solar influence on the lower atmosphere depends on dynamical coupling between different atmospheric layers we also consider some tropospheric signals, where these are linked, and consider how solar forcing influences the atmospheric polar modes of variability. We conclude by presenting a summary of the current understanding of how stratospheric ozone responds to changes in solar activity

Regression technique

Most of the analysis described below has been carried out using a multiple regression technique. The indices used in the regression include representations of some or all of the following features

- a constant, or individual constants for each month to represent the annual cycle;
- a linear trend representing long term climate change;
- a chlorine index;
- solar activity – mainly the 10.7cm solar radio flux;
- the QBO - zonal wind at 40hPa over Singapore;
- ENSO - the “cold tongue” index and
- volcanic aerosol – global average stratospheric aerosol loading as constructed by Sato et al (1993); a background level is assumed since 1996.

Van Loon and Labitzke (1994), reviewing their work up to that date, concluded that a 10-12 year oscillation, in phase with solar activity, occurs over much of the Northern Hemisphere in both the stratosphere and troposphere. They found highest correlations in the summer stratosphere south of about 45ºN, associated with a corresponding periodicity in the temperature of the middle and upper troposphere in the tropics and sub-tropics and deduced that the oscillation is associated with variations in the tropical and sub-tropical circulation. In all their work, however, they used a single linear regression and thus were not been able to estimate the effects of different factors simultaneously influencing the temperature field. This could lead to misattribution of non-solar effects to the sun or, alternatively, to missing solar effects where these interact with the other influences. Most of their studies were also confined to discussions of correlation coefficients and so did not consider the magnitude of the implied solar signals.

By adopting the multiple regression approach the responses to all forcing indices supposed to influence temperature are derived simultaneously. Here we assess the solar contribution, along with the other factors outlined above, to variations in zonal mean temperature in the troposphere and lower stratosphere using the National Centers for Environmental Prediction – National Center for Atmospheric Research (NCEP/NCAR) Reanalysis dataset (http://www.cdc.noaa.gov/cdc/data.ncep.reanalysis.html). We use data only since 1979 as it is well documented (see e.g. Randel and Gaffen, 2000; Haigh 2003) that before that date the lack of satellite data makes the values in the stratosphere unreliable. The annual mean results are shown in Figure 8. There is a clear long-term cooling trend in stratospheric low to mid-latitudes; the characteristic signal of the QBO is displayed in the equatorial stratosphere; ENSO shows a warming of the tropical troposphere a cooling above and a significant warming in the northern polar stratosphere while there is a strong response to the injection of volcanic aerosol – warming the stratosphere and cooling the troposphere. The solar signal shows a statistically significant warming in vertical bands in the mid-latitude troposphere in both hemispheres (discussed previously by Haigh 2003) and a bipolar structure in the lower stratosphere with preferential warming in the sub-tropics (previously noted in ERA-40 data by Crooks and Gray, 2005).

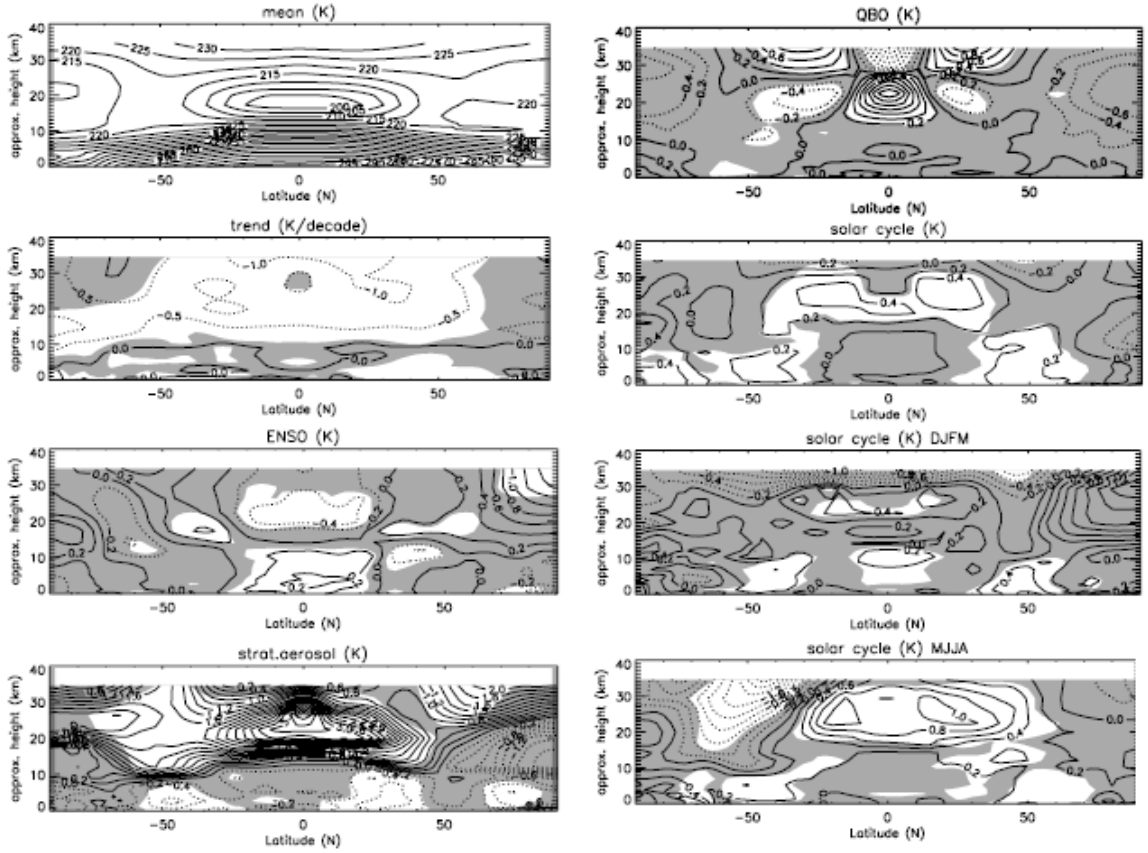

Figure 8: Signals in zonal mean temperature derived from NCEP/NCAR Reanalysis data 1979-2002. The component is identified in the title of each panel. The first six panels relate to the annual mean; the last two are the solar components derived from separate analyses of the DJFM and MJJA seasons. The contour interval is 5K for mean, 0.5 K decade^{-1} for trend, 0.2K all others. Shaded regions are not significant at the 5% level.

The last two panels in Figure 8 show the solar signals derived in separate regression analyses for the solstice seasons, December-March and May-August. Both show the same gross

features seen in the annual mean results (warming bands in the mid-latitude troposphere, bipolar warming in the low to mid-latitude lower stratosphere) although the stratospheric response in much larger in MJJA. The suggestion of a cooling in the mid-to- high latitude middle stratosphere has also been seen in SSU/MSU satellite data (Keckhut et al, 2004). The patterns of response to higher solar activity in both the troposphere and stratosphere suggest that dynamical, as well as direct radiative, factors are taking effect.

Polar modes of variability

The atmosphere exhibits a number of characteristic modes of variability, that are important in determining the local climate in various regions, and it has been suggested that the impact of solar variability, as well as other climate forcing factors, may be to affect the frequency of occupation of certain phases of these modes. Studies of the polar annular modes have suggested that in both Northern (Hartley et al., 1998, Baldwin and Dunkerton, 1999, 2001) and Southern (Thompson et al., 2005) high latitudes variations in the strength of the stratospheric polar vortex often precede similarly signed anomalies in the troposphere. Not all events follow this pattern (Black and McDaniel, 2004), and a chain of causality explaining the mechanisms involved has yet to be established, but the evidence suggests one route whereby any factor (and here, of course, we are specifically interested in solar variability) influencing stratospheric circulations might have an impact on surface climate.

Some authors (e.g. Kuroda & Kodera 1998; Castanheira & Graf 2003) have found evidence of modulation of the NAO by the state of the stratosphere and some (e.g. Kodera 2002; Boberg & Lundstedt 2002; Thejll et al 2003) of a solar signal in the polar modes. All of these studies, however, like Labitzke, have used single linear regression and often confined their discussions to correlation coefficients and so have not considered the magnitude of the implied solar signals in the context of other potential forcing factors.

Here we present a multiple regression analysis of factors potentially influencing the northern and southern annular modes, including the factors outlined above. We investigate levels from the surface to the middle stratosphere and we also conduct a similar analysis of the North Atlantic Oscillation (NAO) in surface pressure, which some authors see as a particular aspect of the NAM but which may alternatively give a more local picture representing synoptic scale variability in the position of the North Atlantic storm track.

The annular mode data used in this study (Mark Baldwin, Northwest Research Associates, USA, personal communication) are based on, at each pressure level, the first empirical orthogonal function (EOF) of 90-day low-pass filtered anomalies, poleward of 20º latitude in each hemisphere, of geopotential heights from the NCEP/NCAR reanalysis. Daily values of the annular mode from 1 January 1958 to 31 December 2001 are obtained by projection of the daily geopotential data onto the EOFs. For further details see Baldwin and Dunkerton (2001) regarding the NAM and Thompson et al. (2005) the SAM. We use monthly averages of the daily values, as we are more interested in the climatological response than in daily development, and we focus on three pressure levels: 1000hPa, 250hPa and 30hPa representing behaviour at the surface, the tropopause and the stratosphere respectively. In the stratosphere we restrict our analysis to data since 1979 because the NCEP reanalysis of the stratosphere is less reliable before this, as mentioned above. At other levels we retain all 44 years of data to provide statistical rigour.

The NAO data used are based on the monthly mean difference in sea level pressure between Gibraltar and South West Iceland as calculated by the University of East Anglia, UK, see http://www.cru.uea.ac.uk/~timo/projpages/nao_update.htm.

No indices representing inter-month variability (annual cycle etc.) are included in the regression analysis as the data are essentially de-seasonalised by the procedure of taking anomalies, as described above. The regression coefficients (β values) for the five varying indices are presented in Table 1. Values assessed to be statistically significant at the 80% confidence level and above are shown in bold type with levels indicated by different colours (see the caption to Table 1). Note that these are regression coefficients, not correlation coefficients; hence the confidence level indicates the importance of the parameters, not the actual size of the coefficients.

Looking first at the results for the NAO we find no significant trend over the period 1958-2001, nor any substantial influence of ENSO. There is a small response to the QBO showing positive NAO anomaly during the QBO-W, but this is not statistically significant. The responses shown to the solar and volcanic forcings, however, are clearly significant at the 95% level; with a positive NAO anomaly shown in response to both higher solar activity and the presence of stratospheric aerosol. While other authors have indicated a link between NAO and solar variability we believe this is the first time that its magnitude has been estimated within a statistically robust framework, taking into account other potential influences.

	pressure (hPa)	**Trend**	**Cl**	**ENSO**	**Vol**	**Sol**	**QBO**
NAO		0.02		-0.09	**0.89**	**0.63**	0.24
NAM	**30**	0.07		-0.22	0.40	0.17	0.22
	250	0.02		**-0.49**	**0.46**	-0.02	0.05
	1000	**0.13**		**-0.53**	**0.53**	0.09	0.20
NAM	**30**	0.05		-0.38	0.67	0.24	0.73
(DJFM)	**250**	0.06		**-1.38**	0.53	0.64	0.39
	1000	**0.23**		-0.82	**1.08**	**0.81**	0.64
SAM	**30**		**0.71**	-0.30	**-0.71**	-0.27	0.31
	250		**0.61**	-0.26	**-0.65**	-0.09	-0.14
	1000		**1.01**	**-0.82**	**-0.65**	-0.04	0.13

Table 1: Regression coefficients for the five standard indices. The data covers the period 1958-2001, except for the 30hPa level for which only values since 1979 are used. Colours indicate the statistical significance levels of the values, derived using a Student's t-test, as follows: 99%, 95%, 90%, 80%, <80%.

The volcanic signal is also seen at 1000hPa in the NAM, although somewhat weaker, but the solar signal has disappeared. If, however, the analysis is carried out using only winter months (average of December to March) there is again a large solar signal (the reduced significance level occurs as a result of the factor 12 decrease in the number of degrees of freedom). A strong ENSO signal is seen in NAM, in both all-month and winter analyses, with a positive ENSO phase being associated with a weaker Arctic circulation, as previously noted by Labitzke and van Loon (1999). No statistically significant solar or QBO signals are found in the stratosphere.

SAM shows a strong correlation with stratospheric chlorine at all levels, indicating a cooling and strengthening of the Antarctic tropospheric polar vortex and confirming the results of Thompson and Solomon (2002). It is also found to be associated with the negative phase of ENSO. No significant response is found to either the Sun or the QBO but a large signal is found of volcanic aerosol of opposite sign to that found in NAM.

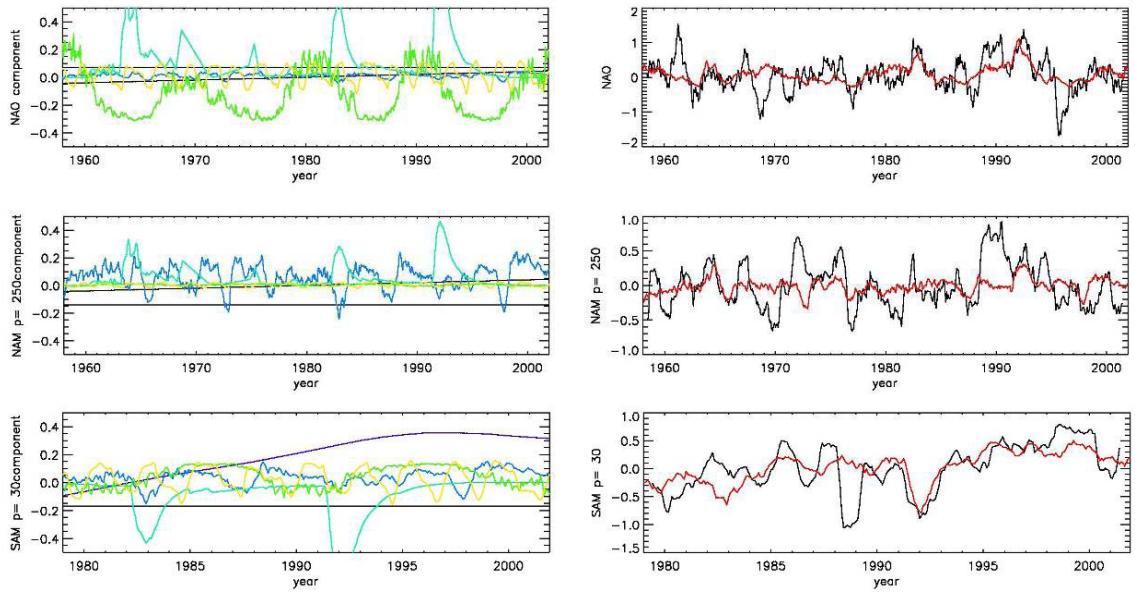

Figure 9: Results of the regression analysis of: Top: NAO; Middle: NAM at 250hPa; Bottom: SAM at 30hPa. The left-hand column shows the time series of the individual components deduced to be contributing to the data. The solar signal is in green, other components as follows: constant (black), linear trend (for NAO and NAM, black), chlorine (for SAM, purple), ENSO (blue), volcanic aerosol (cyan), QBO (yellow). The right-hand column shows the original time series of data in black and the reconstruction from the regression components (without noise component) in red, both smoothed by a 12-month running mean.

A new index

Labitzke and van Loon (1999, LvL) found that the quasi-biennial oscillation modulates the solar signal. By grouping the data according to the phase of the QBO they showed that when it is easterly (QBO-E) the Arctic lower stratosphere is colder when the sun is more active, implying a stronger polar vortex and more positive NAM, but that the opposite holds during QBO-W. More recently Labitzke (2004) has extended this work and shown that introduction of the QBO also aids analysis of northern hemisphere summers, because of changes in global scale Brewer-Dobson circulation, and furthermore that the Antarctic polar vortex is influenced by the solar cycle, modulated by the QBO, in much the same way as the Arctic. This suggests that during QBO-E the SAM is also stronger when the sun is at maximum activity.

Apart from a solar signal in the NAO the responses, shown in Table 1, of the polar modes to solar variability and the QBO appear weak. However, perhaps this is due to the compensating effects described by LvL. To test this out in a statistically robust framework, which avoids the necessity of having to pre-sort data, we define a new regression index composed of the product of the original solar and QBO indices, as shown in Figure 23. Because the original indices were scaled to lie equally about zero their product represents a modulation such that a combination of high solar activity and QBO-W, or low solar activity and QBO-E, has positive values while solar max/QBO-E, or solar min/QBO-W, has negative.

This index has been used in the regression analysis in place of the individual solar and QBO indices. An example of its application is shown in Figure 10 which presents, in the right-hand panel, the amplitude of this index for the zonal mean temperature data in DJFM. The left-

hand panel shows the individual solar cycle and QBO signals from the original DJFM analysis for comparison.

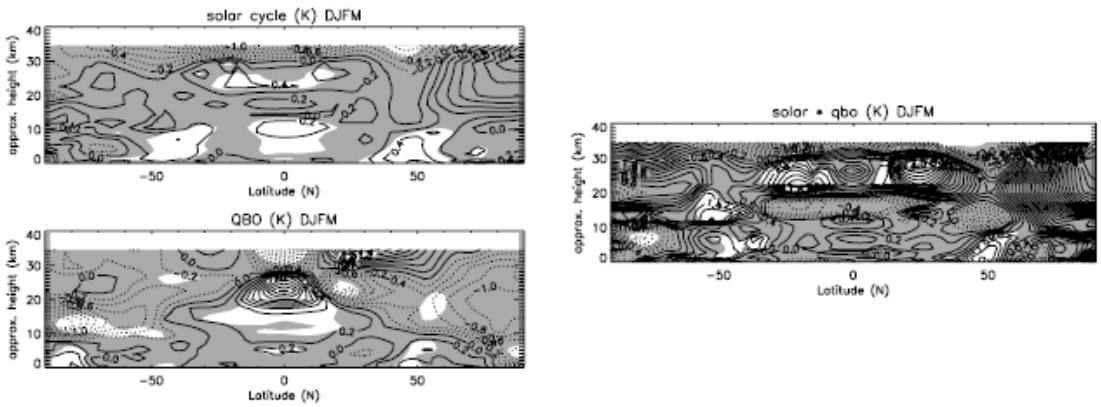

Figure 10: Signal in DJFM zonal mean temperature; left hand side shows results of regression using individual solar and QBO indices (as Figure 8); right hand side shows signal from compound index when this is used in the regression in place of the two original ones.

The regions of significance are still fairly restricted, although with the large internal variability and only 23 data points this is understandable, but it is clear that the signals are much larger than the responses derived for the solar cycle and QBO individually. In the winter polar stratosphere there is a substantial (exceeding 6K) positive response, i.e. the pole is warmer during solar min/QBOE and solar max/QBOW and colder during solar min/QBOW and solar max/QBOE, consistent with the LvL criterion. Signals exceed 2K in the sub-tropical lower stratosphere and 1.5K in the mid-latitude troposphere. This provides significant new evidence that in order to understand solar influences on the lower atmosphere it is necessary to consider dynamical coupling between the stratosphere and troposphere.

	pressure (hPa)	**Trend**	**Cl**	**ENSO**	**Vol**	**Sol*QBO**
NAO		0.03		-0.13	**0.85**	0.11
NAM	**30**	0.05		-0.25	0.40	-0.14
	250	0.02		**-0.47**	**0.45**	-0.16
	1000	**0.13**		**-0.52**	**0.50**	-0.27
NAM	**30**	0.02		-0.47	0.73	-0.13
(DJFM)	**250**	0.07		**-1.39**	0.38	**-0.91**
	1000	**0.24**		-0.85	0.96	**-1.16**
SAM	**30**		**0.78**	-0.27	**-0.76**	**-0.53**
	250		**0.61**	-0.17	**-0.71**	**-0.57**
	1000		**1.01**	**-0.71**	**-0.75**	**-0.89**

Table 2: As Table 1 for values derived using the compound solar*QBO index in place of the solar and QBO indices independently

The derived regression coefficients for the annular modes derived using the composite index are presented in Table 2. The first thing to note is that the values for the trend/chlorine, ENSO and volcanic signals are very similar to those in Table 1: this provides evidence of the

independence of the indices and the robustness of these signals. The right-hand column of Table 2 shows all negative values (except for the NAO) consistent with the Labitzke criterion stated above. The signals in NAM (except at 30hPa) and in SAM are larger in magnitude than the individual solar and QBO signals in Table 1 and generally statistically more robust. This is particularly true of SAM for which a strong signal emerges at all levels where very little was shown for the individual indices.

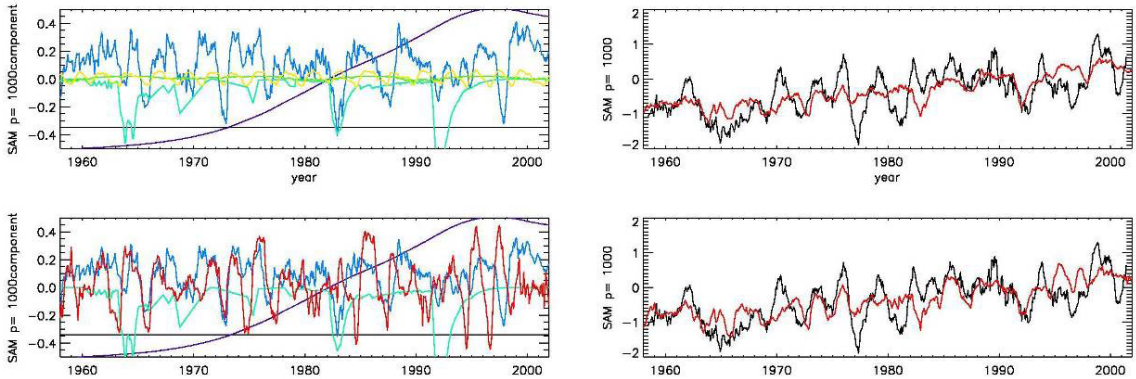

Figure 11: Results of the regression analysis of SAM at 1000hPa. The left-hand column shows the time series of the individual components deduced to be contributing to the data. The top row presents the results using the original indices (colours as in Figure 9 with the solar signal in green); the lower row shows the results using the compound (Solar x QBO) in place of the solar and QBO indices individually, with the compound index in red and other indices unchanged. The right-hand column shows the original time series of data in black and the reconstruction from the regression components (without noise component) in red, both smoothed by a 12-month running mean.

As an example the time series of the derived components of SAM at 1000hPa, and of the original and reconstructed data, are presented in Figure 11. The amplitude of the composite component is clear in the lower left-hand panel of this Figure and the right-hand panels show that the reconstructed time series is able to reproduce more of the variance in the original data than could be achieved with the original components.

Summary

Our studies of the NCEP/NCAR Reanalysis dataset show signals in response to the solar cycle in zonal mean temperatures and winds throughout the troposphere and stratosphere and in all seasons. The clearest patterns to emerge are warming of around 0.5K (in solar max relative to solar min) in the low to mid-latitude lower stratosphere with largest values in the sub-tropics and northern hemisphere summer and vertical bands of warming, of a few 1/10ths K, in the mid-latitude troposphere. The winter polar stratospheric jet moves equatorward while the summer stratospheric easterlies weaken; in the troposphere the winter sub-tropical jets weaken and the mid-latitude jets move poleward. There is a clear solar influence detected in the NAO, consistent with the strengthening of the winter westerlies near 50ºN, but no statistically significant signals of solar forcing are found in either the NAM or SAM.

Based on Labitzke and van Loon's findings concerning the combined influence of solar activity and the phase of the QBO on polar meteorology we have defined a new regression index, the product of the solar and QBO indices. When this is used is used in place of the two factors individually then several other features appear. Firstly, as expected, a strong signal in winter polar stratospheric temperatures, as identified by Labitzke and van Loon but we are now able to place these findings within a statistically robust framework and to assess the magnitudes of the effects in the presence of influences by other factors such as volcanic

eruptions and ENSO. We also find that the magnitudes of the temperature signals in the tropical lower stratosphere and mid-latitude troposphere are considerable larger than derived using the solar and QBO indices separately.
A strong influence of the composite index is found throughout the atmosphere in the SAM which showed very little solar or QBO signals in the original analysis. The signal in winter NAM is also increased. Perhaps surprisingly our results for the polar modes show more significance in the troposphere than the stratosphere, but this may be due to the necessity of using a shorter time series at higher altitudes because of the unreliability of the reanalysis datasets in the stratosphere before the inclusion of satellite data.
The NAO behaves differently to the NAM (and SAM) in that the signal found for the combined solar*QBO index is in a different sense to that found in the other modes and also of smaller magnitude than that found for the single solar influence in the original analysis. We tentatively conclude that solar variability influences NAM and SAM through its impact in the polar stratosphere, modulated by the QBO, whereas the solar influence on the NAO is the result of a different process. Our previous work (Haigh 1999, Larkin et al 2000, Haigh et al 2005) suggests this may involve changes in the tropospheric Hadley circulation and storm tracks resulting from solar heating of the tropical lower stratosphere but the mechanisms whereby all these processes take place remain to be elucidated.
A signal in low latitude ozone column of about 3% peak-to-peak over the solar cycle is becoming better established as the lengths of the data series extend. However, substantial uncertainties still remain in the response of ozone vertical profiles to solar variability with reservations concerning both observational data analyses and model simulations.

4 Tropospheric Interactions

In the following we describe the most prominent results of our correlation study of between solar output/solar modulated parameters and the troposphere. We first briefly review our method of analysis.

Method of analysis

In the correlation study we focused on 5 external forcing parameters that are modulated by solar variability and have the potential to influence Earth's lower atmosphere below 50km: 1) Total Solar Irradiance (TSI, 1978 – 2005), 2) Ultra-Violet (UV, 1978 – 2005), (prior to 1978, 10.7 cm radio flux proxy for the Extreme Ultra-Violet (EUV), 3) Galactic Cosmic Rays represented by the neutron counts at Climax (GCR, 1953-2005), 4) Solar Wind, represented by the product between the solar wind speed, v_{sw}, and the southward component of the IMF (SW, 1963 to 2005), and 5) total Hemispheric Power Input, indicating the amount of energy deposited over an entire hemisphere in the upper atmosphere by precipitating particles (HPI,1978-2003).
As it was noted in the Introduction there is little difference in the phase between the various solar modulated forcing parameters over a solar cycle. As a result, it is difficult to determine the solar modulated process responsible for any significant response found in the climate data at time scales where the effects of the solar cycle dominate. In an attempt to tackle the problem of the dominating solar cycle, the effects of the solar cycle were removed from the data using two techniques;

1) via multiple-regression where the solar cycle is represented by the sunspot number. In general, we made three sets of correlations for each pair of solar-climate parameters: with raw data; removing linear trends (also internal modes of

variability from the climate data, see below); removing the solar cycle. Representing the solar cycle by the sunspot number was an arbitrary choice. Any parameter representing the overall activity of the Sun would be usable.

2) by selecting narrow periods around solar max and solar min where the effects of the solar cycle are almost stationary (not included in this report).

This allowed for a comparison of fluctuations in the data at higher frequencies than the solar cycle. A cursory glance at the solar modulated forcing parameters indicates that the amplitudes of fluctuations around the solar cycle are much larger under solar maximum than solar minimum conditions. These fluctuations, which are generally independent for each forcing parameter, e.g., Forbush decreases, ground level events, solar flares etc., provide a possible means to distinguish between the different processes. However, the solar processes are highly variable at time-scales of hours to days. This makes the task of identifying a solar signal in the climate data more involved since, at these timescales, fluctuations in local weather phenomena and internal climate variations are often large and can mask the solar effect being explored. This is likely to have a strong impact on the data analysis. So there is a trade-off between the need to resolve short term fluctuations, possibly driven by solar variability, above the internal noise of the climate system. The data used in the following analysis is therefore limited to monthly averages, which reduces the climatic noise, but also allows for an analysis of high frequency fluctuations around the solar cycle.

The effect of the solar cycle on these five parameters is clearly visible from the correlation coefficients, (Table 3), with sunspot number (SSN). Also indicated are the correlation coefficients between the five solar modulated parameters before removal of the solar cycle (above the diagonal, bold face), after removal of the solar cycle (below the diagonal, normal type), and between each solar modulated parameter before and after removal of the solar cycle (diagonal, italics).

Note that SW and in particular HPI, display the weakest correlation with both SSN and the other parameters.

	TSI	UV	EUV	SW	HPI	GCR	SSN
TSI	*0.70*	**0.80**	**0.79**	**0.31**	**0.09**	**-0.63**	**0.72**
UV	0.59	*0.30*	**0.98**	**0.48**	**0.17**	**-0.79**	**0.77**
EUV	0.50	0.77	*0.27*	**0.50**	**0.19**	**-0.85**	**0.96**
SW	-0.02	-0.06	0.07	*0.87*	**0.59**	**-0.54**	**0.46**
HPI	-0.03	0.04	0.14	0.60	*0.99*	**-0.44**	**0.15**
GCR	-0.21	-0.44	-0.42	-0.29	-0.53	*0.61*	**-0.79**

Table 3: Correlation coefficients between the solar modulated forcing parameters. Above the diagonal (bold face) is given the correlations for the observed parameters. Below the diagonal (normal type) the same coefficients after removal of linear trend and the solar cycle from the parameters are shown. The diagonal shows the correlations for each parameter before and after removal of the solar cycle and linear trend.

Another important consideration is the effect of internal climate variability at decadal time scales and the impact from volcanoes. Since these processes can have a strong impact on many climate parameters in the troposphere and at the surface, they could mask, or artificially enhance, a possible solar cycle signal with an average length around 11 years. To reduce this problem, temporal indices describing the variability from El

Nino Southern Oscillation (ENSO), North Atlantic Oscillation (NAO) and Volcanic Stratospheric Aerosol have also been included in the multiple regression analysis.

Temperature

Reliable measurements of atmospheric temperatures at other levels than ground have been collected from balloon radiosonde measurements since 1958, beginning with observations from a few stations reaching thousands of stations at the present time. The Hadley Centre of Climate Prediction and Research has compiled the radiosonde temperature measurements into a gridded data set from 1958 to present. The data are available as monthly temperature anomalies at 9 pressure levels [850, 700, 500, 300, 200, 150, 100, 50, 30hPa] on a 5-degree latitude and 10-degree longitude grid. For the analysis in this section the internal modes of variability have been subtracted from the temperature data by multi-linear-regression and the temperature data been recomputed as latitude zones containing monthly means of the anomalies

Global averages

The global average of the temperature in the troposphere is here defined as the average of the lowest 4 levels from the balloon radiosonde measurements (850 hPa – 300 hPa). Below, in Figure 12, we show the correlation between global tropospheric temperature anomalies and EUV radiation and galactic cosmic rays. In the top panels are shown the raw data giving correlations of 0.33 with EUV and –0.31 with GCR. In the temperature the effect of particularly the El Niño is clearly seen. In the middle panels the internal climate modulators, NINO3, NAO, and VAI have been removed from the temperature together with a linear trend by linear regression. A linear trend has also been removed from the GCR and EUV curves. The correlation coefficient grows somewhat to 0.42 and –0.47. The improved correlation is clearly seen by visual inspection. However, since all the external parameters are strongly modulated by the solar cycle, it is not at all obvious how to distinguish coincidental correlation from actual physical influence. In the bottom panel we have therefore removed the solar cycle, represented by the monthly sunspot number, from both the temperature and the external parameters. The correlation drops significantly, most dramatically for the EUV-temperature correlation. In Table 4 we give the correlations for all 5 external parameter for raw data, with NINO3, NAO, VAI, and a linear trend removed, and with the solar cycle removed. The numbers in parentheses are the same correlation coefficients but after a 3 months box average has been applied. Particularly, TSI, EUV, and GCR show strong correlations. However, these correlations drop significantly after removal of the solar cycle. Only the GCR correlation survives to some extent.

One must bear in mind that the correlations for the various parameters are not calculated over the same time period. TSI and HPI are only available from November 1978. In Table 5 we show the correlations if we limit the analysis for all the parameters to this period. The correlations for UV, SW, GCR, and SSN drop. In fact, only the correlations for UV and SSN are above the 95% significance level after removal of the internal modes of variability. After removal of the solar cycle none of the parameters show any correlation.

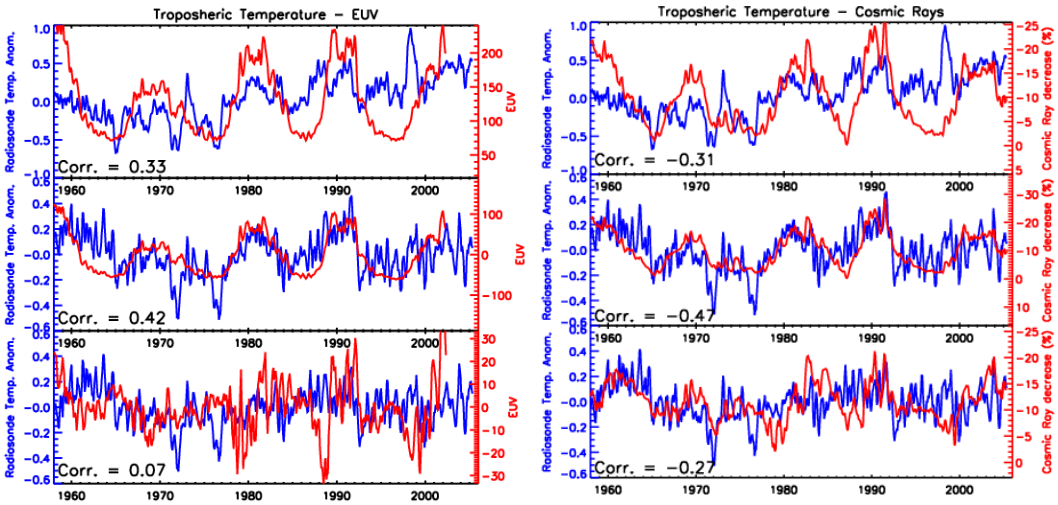

Figure 12: Left) correlation between 10.7 cm EUV proxy and global mean temperature anomalies for the troposphere. Top panel: observations. Middle panel: after removal of nino3, NAO, volcanic aerosols, and a linear trend. Bottom: after removal of the solar cycle. Right) the same for galactic cosmic rays.

	TSI	EUV	SW	HPI	GCR	SSN
Observ.	0.13 (0.16)	**0.33 (0.35)**	**0.20 (0.31)**	-0.08 (-0.07)	**-0.31 (-0.33)**	**0.25 (0.27)**
Niño, etc.	0.31 **(0.44)**	***0.42 (0.50)***	0.19 **(0.35)**	0.07 (0.14)	***-0.47 (-0.57)***	***0.40 (0.48)***
Solar cycle	0.05 (0.00)	0.07 (0.07)	-0.02 (0.02)	-0.01 (0.03)	**-0.27 (-0.33)**	

Table 4: the correlations coefficients for the 5 external parameters with tropospheric temperature. Given are the correlations for raw observation, after removal of the internal climate parameters, and after removal of the solar cycle. Numbers in bold face are above the 95% significance level. Numbers in bold italics are above the 99% significance level.

	TSI	UV	SW	HPI	GCR	SSN
Observ.	0.13 (0.16)	0.18 (0.21)	0.06 (0.08)	-0.08 (-0.07)	-0.16 (-0.18)	0.12 (0.14)
Niño, etc.	0.31 (0.44)	**0.39 (0.50)**	-0.13 (-0.23)	0.07 (0.14)	-0.22 (-0.27)	***0.42 (0.54)***
Solar cycle	0.05 (0.00)	0.04 (0.03)	-0.06 (-0.06)	-0.02 (0.03)	-0.05 (-0.04)	

Table 5: same as Table 4, but limited to the period November 1978-present.

Zonal averages

The various external parameters may influence different parts of the globe differently, both geographically and at different altitudes. Below we analyse the correlations with zonal averages of temperature anomalies given by balloon radiosonde measurements at nine different altitude levels (850 hPa – 30 hPa).

In Figure 13 we illustrate the analysis for the GCR parameter. For the raw observations (top, left) a clear correlation is seen in the troposphere, particularly strong in the tropical region, but without much signal in the stratosphere. After removal of the internal climate parameters (top right) the region of strong correlation extends into the stratosphere. However, after removal of the solar cycle (bottom, left) most of the correlations disappear. The correlation with the solar cycle (bottom, right) displays very much the same pattern as the GCR correlation before removal of the solar cycle. The zonal correlations with GCR are made for the full time period 1958-present.

Figure 14 shows the zonal temperature correlations with the external parameters after removal of the solar parameters. None of the parameters displays correlations comparable

to those between temperature and sunspot number, though GCR and EUV do show some areas with significant correlations.

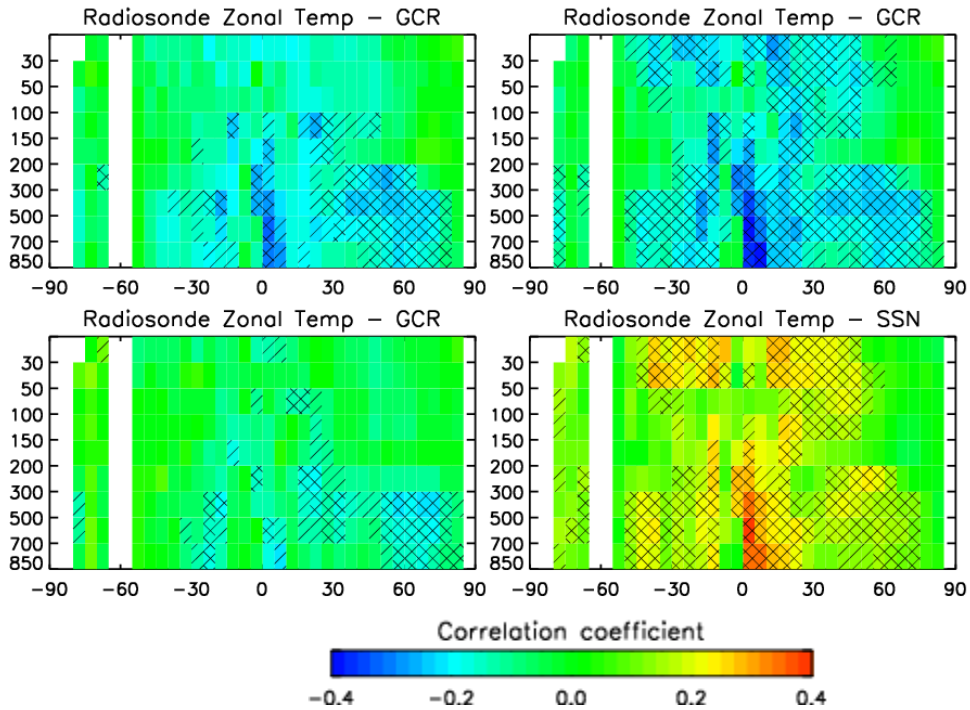

Figure 13: zonal correlations between GCR and radiosonde temperatures. Top left: raw observations. Top right: after removal of nino3, NAO, VAI, and linear trend by linear regression. Bottom left: after removal of the solar cycle. Bottom right: zonal correlation between sunspot number and radiosonde temperatures. Hatched areas have correlations above the 90% significance level, cross hatched above 95%.

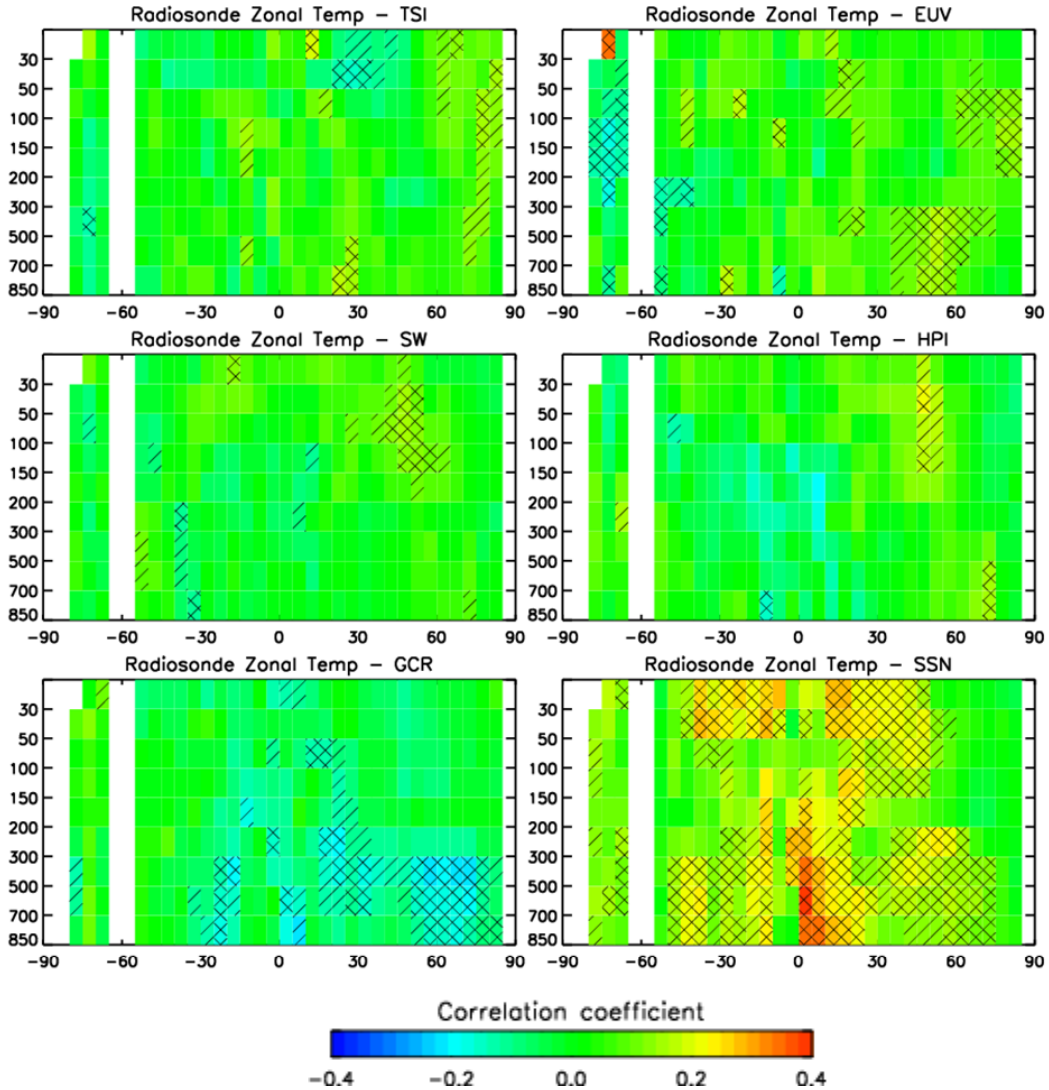

Figure 14: zonal correlations between the 5 external parameters plus the sunspot number and radiosonde temperature anomalies. The correlations are calculated after removal of the solar cycle. From top TSI and EUV, SW and HPI, GCR and SSN. Hatched areas have correlations coefficients above the 90% significance level, cross hatched above 95%.

Low clouds

Low clouds are taken from the ISCCP cloud data sets which have recently been updated to provide a systematic view of global cloud behaviour over the period July 1983 – December 2005. ISCCP initially divides the clouds into three types based on altitude, low, middle, or high, using either infrared or a combination of infrared and visual observations. The analysis here is restricted to low clouds derived from infrared observations only. Previous work has suggested that a problem with the continuous calibration exists at the end of 1994 and beginning of 1995, most easily noticed in the high cloud cover where a clear drop of more than 1% in global high cloud coverage is reported at the end of 1994. At the end of 2001 the high cloud coverage comes back up to the level pre-1995. Comparison with an independent data set of low cloud provided by the SSM/I microwave instrument aboard the DMSP satellites suggest that there is an

offset between these two data sets. Following the procedure of Marsh and Svensmark (2003) the ISCCP low cloud data has been adjusted to account for this offset at every grid point after 1994. Below the analysis from both the original and adjusted data is presented.

Tables 6 and 7 report the correlation coefficients between all 5 solar modulated parameters and low clouds (original and adjusted respectively). A key feature is that the strongest significant correlations are found with UV and GCR, both with and without the inclusion of the solar cycle. For the original observed data in Table 6 UV displays the strongest correlation, however, after filtering out internal climate modes GCR becomes slightly stronger. For the adjusted data in Table 7 correlation coefficients with GCR are actually slightly stronger than UV for both the observed and filtered data. The strong correlation with SSN indicates that a large fraction of these strong correlations are due to the solar cycle, however, a significant correlation still exists in UV and GCR once the solar cycle is removed. This displays the most consistent feature since both in the original and adjusted data it is the UV that possesses the strongest significant correlation.

	TSI	UV	SW	HPI	GCR	SSN
Observ.	-0.40(-0.46)	**-0.58(-0.62)**	-0.24(-0.37)	-0.08(-0.11)	0.40(0.43)	-0.36(-0.40)
Niño, etc.	**-0.41(-0.50)**	***-0.50(-0.57)***	-0.24**(-0.42)**	**-0.31(-0.43)**	***0.52(0.61)***	-0.42(-0.50)
Solar cycle	**-0.21**(-0.24)	***-0.50(-0.60)***	-0.07(-0.17)	-0.18(-0.27)	**0.35(0.41)**	

Table 6: the correlations coefficients for the 5 external parameters and the sunspot number with low cloud coverage. Given are the correlations for raw observation, after removal of the internal mode of variability, and after removal of the solar cycle. Numbers in bold face are above the 95% significance level, numbers in bold italics above the 99% significance level.

	TSI	UV	SW	HPI	GCR	SSN
Observ.	**-0.54(-0.67)**	**-0.61(-0.71)**	**-0.34*(-0.57)***	-0.30**(-0.40)**	**0.62(0.72)**	-0.57(-0.68)
Niño, etc.	-0.49**(-0.63)**	**-0.57(-0.68)**	-0.27**(-0.49)**	-0.28**(-0.39)**	***0.59(0.71)***	**-0.54(-0.67)**
Solar cycle	**-0.23**(-0.26)	***-0.41(-0.47)***	-0.03(-0.13)	-0.10(-0.17)	***0.32*(0.39)**	

Table 7: same as Table 6, but after adjustment with the SSM/I DMSP cloud data.

Figure 15 shows a plot of UV (green) and GCR (red) together with the original (left) and adjusted (right) globally averaged low cloud data (blue). The correlation over nearly two and a half solar cycles is quite striking, particularly once the internal climate modes have been filtered out. The spatial distribution of correlation coefficients once the solar cycle has been removed (Figure 16) indicate that the strongest significant correlations are found at mid to high latitudes for both UV (negative) and GCR (positive). However, there also exist regions of positive (UV) and negative (GCR) correlation around the equator, particularly for GCR, which are washed out when taking the global average

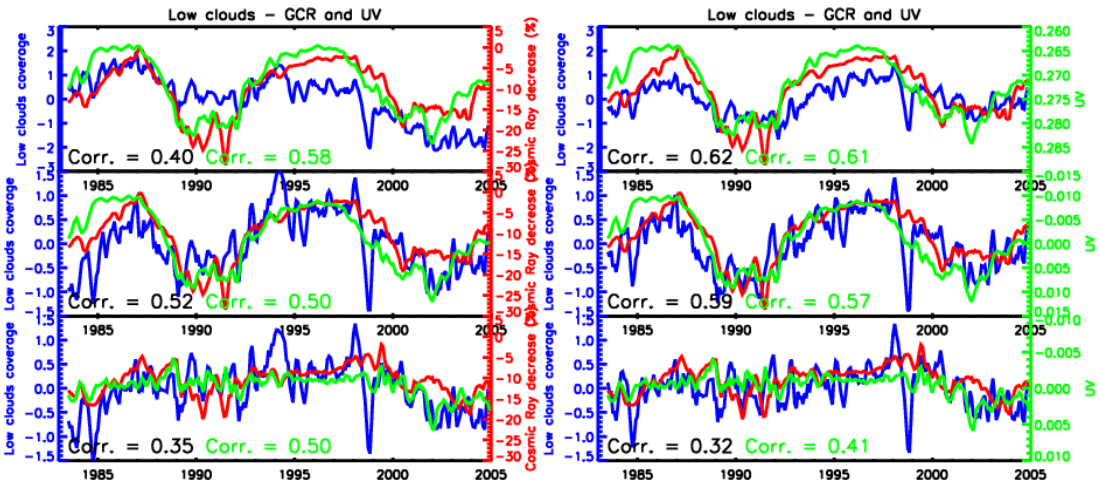

Figure 15: Correlation between GCR (red) and UV (green) and coverage of low clouds (blue). Left: ISCCP data for coverage of low altitude clouds. From top: annual cycle removed, trend and internal modes removed, solar cycle removed. Right: same as left, but after adjustment with the SSM/I DMSP cloud data.

Summary

No single solar modulated parameter consistently dominated the response found in each of the climate parameters investigated in this report. The clear majority of solar modulated variability in the various climate parameters could be explained by effects related to the solar cycle. However, some significant differences in the strength, sign and spatial distribution of the correlation became apparent once the effects of the solar cycle had been removed.

The main highlights from the correlation study, once the solar cycle had been accounted for, can be summarised for each of the solar modulated parameters as follows:

TSI

- Zonally averaged temperature under solar min conditions showed some significant positive correlation in the equatorial troposphere.
- No significant correlation was found in any of the other climate parameters.

UV

- Zonally averaged temperatures displayed significant positive correlation coefficients that were comparable to those found with GCR, but then disappeared after removal of the solar cycle.
- Zonally averaged temperatures under solar max/min conditions show a negative/positive correlation in the troposphere, similar, but weaker than, the feature found with GCR.
- Low clouds displayed negative bands of correlations at mid to high latitudes. These bands were *strengthened* by removal of the solar cycle leading to additional positive bands of correlation to appear in the tropics.

- Ozone displayed limit areas that were correlated with UV but these were significantly stronger than with the other solar modulated parameters.
- Aerosols displayed a significant positive correlation in the southern hemisphere.

SW

- Zonally averaged temperature under solar min conditions showed some significant positive correlation in the stratosphere.
- No significant correlation was found in any of the other climate parameters.

HPI

- Zonally averaged temperature under solar min conditions showed some significant negative correlation in the equatorial troposphere.
- Aerosols displayed a significant positive correlation at the equator.
- No significant correlation was found in any of the other climate parameters.

GCR

- Zonally averaged temperatures displayed a significant negative correlation. GCR was the only parameter displaying a significant correlation for global averages after removal of the solar cycle. However, when limiting the analysis to data after 1978 this correlation disappeared.
- Zonally averaged temperatures under solar max/min conditions show a negative/positive correlation in the troposphere. A similar, but weaker, feature was found with UV, but did not appear with any of the other solar modulated parameters.
- Low clouds displayed negative(positive) bands of correlations at mid to high latitudes similar to UV. The response with UV and GCR was generally very similar and it was difficult to distinguish between these two parameters. However, after removal of the solar cycle the globally averaged correlations were definitely weaker for GCR.
- Aerosols displayed a significant correlation in the southern hemisphere which could not be distinguished from the signal found with UV.

Two final features of note are:

1) That the vertical circulation displayed significant latitudinal bands of positive and negative correlation with all solar modulated forcing parameters after the solar cycle had been removed. However, the latitudinal position of these bands was different for each parameter.
2) Virtually no significant correlation was found in any of the surface climate parameters.

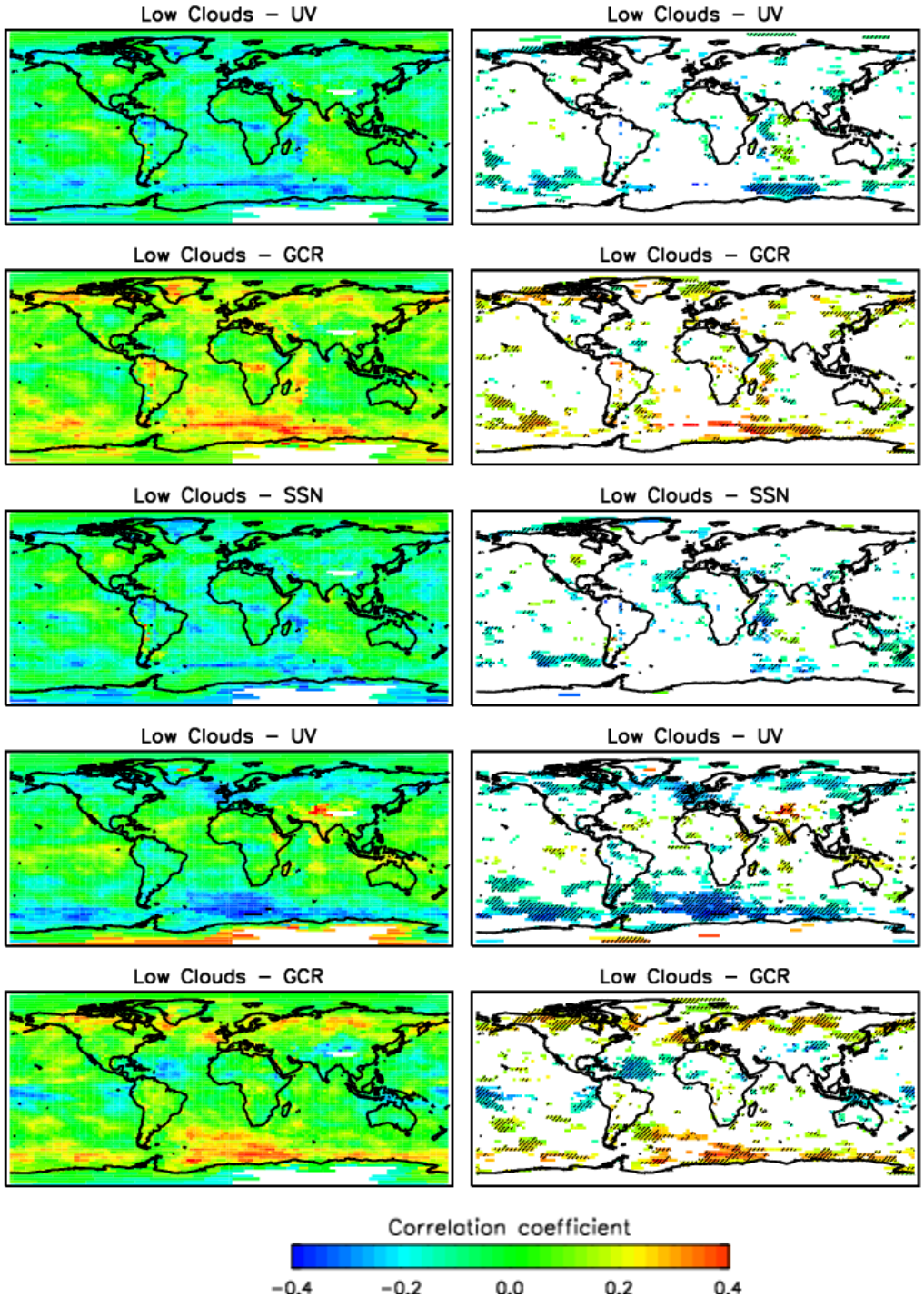

Figure 16: correlations between the UV and GCR plus the sunspot number and coverage of low clouds. The top two rows show the correlations with UV and GCR before the solar cycle is removed; third row shows the correlation with sunspot number; two bottom rows show the UV and GCR correlations after the solar cycle is removed. Some strong contrasts, for example in the Indian Ocean east of Africa are the effect of the foot point of the observing geo-stationary satellites. To the right are shown only the areas with correlations above the 90% significance level, hatched areas are above 95% significance.

5 Mechanisms

Though a solar signal is evident in many climate parameters, and though it is obvious that the Sun drives Earth's climate, the exact physical mechanisms by which solar variations manifest themselves in the climate system is yet poorly understood. One reason is that it is difficult, if not impossible, to separate each solar driver, e.g., TSI, UV, modulation of cosmic rays, and pinpoint it to a single climate response.

A key concept in the area of climate change is that of "Radiative Forcing". This is loosely defined[2] as the instantaneous net radiative imbalance at the top of the atmosphere introduced by some perturbing factor. The latter could be a change in atmospheric composition or incoming solar irradiance or of the Earth's albedo. Radiative forcing is a useful concept as it gives a top level indication of the potential impact of the perturbing factor on the equilibrated global mean surface temperature of the Earth. Because of this it is used extensively to indicate the relative impacts of various anthropogenic and natural factors on climate. In the Fourth Assessment Report of the Intergovernmental Panel on Climate Change (IPCC, 2007) the solar contribution is perceived to be very small, but the ascribed "Level of Scientific Understanding" is low.

Below we summarize current understanding of the physical mechanisms responsible for the solar signals in the atmosphere with an emphasis on UV, TSI, and cosmic rays.

Solar signals through the stratosphere and troposphere

A number of analyses now indicate a statistically significant signal of solar cycle variability in a range of meteorological parameters throughout the stratosphere and troposphere. Early work indicating correlations between solar activity and lower atmospheric temperatures was presented by Labitzke and van Loon (1995). More recently the availability of reanalysed datasets from the US National Centre for Environmental Prediction (NCEP) and the European Centre for Medium Range Weather Forecasts (ECWWF) has provided global data over a forty year period for climate studies. These have allowed some rigorous analysis of solar signals. Temperatures show not the uniform warming that might be expected when the Sun is more active but statistically significant warmer regions in the low latitude upper and lower stratosphere, and in the subtropics to mid-latitudes extending throughout the lower stratosphere and troposphere. The corresponding zonal wind fields indicate that the mid-latitude tropospheric jets are weaker and displaced slightly towards the poles at maxima of the solar 11-year cycle relative to the minima. The influence on surface winds at high latitudes can also be seen in terms of the polar modes of variability. Boberg and Lundstedt (2002) have shown a correlation between the North Atlantic Oscillation and the electric field strength of the solar wind. In a different study of the Northern Annular Mode we also found that it varied with solar activity but that the combined influence of the Sun and the quasi-biennial oscillation in tropical stratospheric winds provided a better indicator of the strength of the circumpolar circulation in both northern and southern hemispheres (see Table 8). As well as signals in temperature zonal wind studies have indicated a solar signal in the mean overturning circulation of the atmosphere.

[2] More precisely radiative forcing is defined as the change in net radiative flux at the tropopause after allowing for stratospheric temperatures to readjust to radiative equilibrium but with surface and tropospheric temperatures held fixed.

	Trend	Cl	ENSO	Vol	Sol	QBO	Sol*QBO
NAM (DJFM)	**0.23**		-0.82	**1.08**	**0.81**	0.64	
	0.24		-0.85	0.96			**-1.16**
SAM		**1.01**	**-0.82**	**-0.65**	-0.04	0.13	
		1.01	**-0.71**	**-0.75**			**-0.89**

Table 8: Multiple regression analysis of the Northern Annular Mode at the surface in winter and of the Southern Annular Mode at the surface. Columns show regression coefficients for linear trend (N.H. only), stratospheric chlorine (S.H. only), El Niño-Southern oscillation (ENSO), volcanic (stratospheric) aerosol loading, solar variability (10.7cm index) and the quasi-biennial oscillation (QBO). The column labelled Sol*QBO indicates that an index composed of a product of the solar and QBO indices was used in place of those two factors individually. The data cover the period 1958-2001. Colours indicate the statistical significance levels of the values, derived using a Student's t-test, as follows: 99%, 95%, 90%, 80%, <80%. (Haigh and Roscoe, 2006)

Solar variability and stratospheric ozone

The influence of solar variability on stratospheric ozone is important because this will impact both the temperature of the stratosphere (with implications for stratosphere-troposphere coupling – see below) and radiative forcing of the troposphere. However, the 11-year cycle in ozone remains poorly characterised. Results from satellite data appear to show a minimum in the ozone profile near 30km which is not seen in model simulations. The importance of the ozone change in determining the radiative forcing is illustrated in Figure 63.

Evidence for stratosphere-troposphere coupling

There is some observational evidence that variations in the strength of the polar vortex in the upper stratosphere may subsequently influence surface climate. A study of polar temperature trends by Thompson and Solomon (2005) also suggests a downward influence and modelling experiments by Gillett et al (2004) demonstrate that depletion of stratospheric ozone over the South Pole can affect the troposphere after about one month. None of these studies is specifically concerned with a solar influence but the accumulating evidence suggests that any factor influencing the strength of the polar stratospheric jet may be able to influence surface climate. The original modelling study of Haigh (1996) showed, using an atmospheric GCM with fixed sea surface temperatures, that changes in solar UV produced a weakening and poleward shift of the mid-latitude jets. These changes are similar in sense, though of a somewhat smaller magnitude to those found in NCEP data analysis. The Haigh (1996) model also showed a weakening and broadening of the tropical Hadley cells (mean meridional overturning) at solar maximum. This experiment was repeated using an entirely different model by Larkin et al (2000) with similar results in all seasons.

Mechanisms of stratosphere-troposphere coupling

While some of the similarities between the observational analyses of solar influence and modelling studies of UV effects are intriguing they do not explain the mechanisms whereby the influence takes place. In a series of papers Kodera has argued that changes in the winter polar stratospheric brought about by anomalous solar heating may influence the passage of upward propagating planetary waves and thus their deposition of momentum and hence the strength of the mean overturning of the stratosphere (aka the Brewer-Dobson circulation). An alternative (or additional?) perspective is provide by the

work of Gray and co-workers who have demonstrated using rocketsonde and satellite data that zonal wind anomalies in the tropical upper stratosphere are correlated with subsequent temperature anomalies in the polar lower stratosphere. They also demonstrated this effect in a mechanistic model of the middle atmosphere. The Kodera and Gray studies provide evidence and mechanisms whereby solar perturbations to the upper stratosphere may affect the lower stratosphere, in both cases enhancing any direct solar heating in this region. However, they do not explain the apparent subsequent propagation downwards into the troposphere.

Role of Ionisation

Ions produced through the nucleonic cascade of cosmic rays in the troposphere rapidly interact with atmospheric molecules and are converted to complex cluster ions (Gringel et al. 1986; Hoppel et al. 1986). There are two loss terms for the ions; ion-ion recombination and ion-aerosol attachment. Ion production rates in the lower troposphere mean that the average lifetime of a small ion is up to 350 s. The ions act as charge carriers in the Global electric circuit which can generate charge build-up at cloud boundaries, and affect the processing of CCN/cloud droplets (Electroscavenging). Ions are also thought to play a role in stabilizing an initial atmospheric cluster until it is large enough to continue growing via neutral growth mechanisms into a particle/CCN (Ion Induced Nucleation). In addition, ions will attach to pre-existing aerosol nucleated through neutral processes, once charged there is a potential the aerosol's continued growth is enhanced (Charge Assisted Growth). These mechanisms are likely to have an impact on the number of aerosols acting as cloud condensation nuclei (CCN) at typical atmospheric super-saturations of a few percent [Viggiano and Arnold 1995].

It is currently an open question as to how the initial clusters are stabilized until they reach this critical size. One mechanism that has been gaining increasing attention is the role of ionization during the early stages of nucleation, known as Ion Induced Nucleation (IIN). Since the majority of atmospheric ions are generated by cosmic rays, IIN processes could be important for understanding a sun-climate link.

A number of theoretical models have been developed to explore IIN, and there are currently two models of particular note (Yu and Turco, 2000; Yu, 2006), and (Lovejoy et al 2004). Although the models of Yu and Lovejoy are similar, there is a major difference. Yu's model predicts significant growth of the cluster ions before recombination under lower Tropospheric conditions (potentially important for low clouds – see later) which provides a significant source of new particle generation in the presence of ionisation. However, under similar conditions Lovejoy's model only finds a negligible contribution to nucleation from ions, but a relatively large contribution at mid-upper Tropospheric conditions. This appears to be a result of differences in the physical description of the cluster thermodynamics, and the treatment of positive ions which are explicitly allowed to evolve by Yu, but treated as a single species restricted to small ions in Lovejoy's model. However, there are large uncertainties in both these processes due to a lack of rigorous experimental data and lack of a suitably robust theoretical description of cluster thermodynamics that are valid under a wide range of atmospheric conditions. Both models indicate that, based on current nucleation theory, there is a significant role for ionisation in the nucleation of new particles in the atmosphere, but that it is unclear as to where in the atmosphere the largest contribution should be expected.

Low clouds

Yu's model suggests that CCN in the lower troposphere and marine boundary layer (below 5 km) are most sensitive to changes in ionisation. Under such conditions, an increase in GCR would lead to an increase in the number of aerosols, CCN and cloud droplets and hence a decrease in cloud droplet sizes. Ferek et al. (2000) have shown that an increase in aerosol concentrations due to ship exhaust can lead to drizzle suppression. This clearly has an impact on cloud microphysics and in turn implications for cloud properties. However, ship tracks are a large perturbation locally, whereas a possible GCR - CCN mechanism will be a small perturbation globally. If ionization from GCR can be shown to have a similar affect on the lower tropospheric aerosol distribution, and subsequently prolong a cloud's lifetime, it would be consistent with the cosmic ray - low cloud correlation (Marsh and Svensmark, 2000). An effect from ionisation on clouds would provide the link to climate with their strong impact on the radiative budget of the Earth.

Role of TSI

The total solar irradiance (TSI) is in a sense the most obvious solar parameter to single out for study when considering the Sun-climate connection. The power input received by the Earth from the Sun is the driver of Earth's climate system and the variations in TSI do correlate reasonably well with the variations seen in the climate. However, the brute variations in power received at Earth are not strong enough to explain the variations in climate that are observed. Variations in TSI over a solar cycle of 1.3 W/m^2 at the top of the atmosphere translates to 0.23 W/m^2 at the surface. With a climate sensitivity of 0.5-0.8 $K/(W/m^2)$ this corresponds to a change in tropospheric temperature of 0.14-0.18 K. The observed variations in tropospheric temperatures over a solar cycle are, however, approximately 0.5 K. For TSI to be the driver of the climate variations observed some sort of amplification or feedback mechanism must therefore be in place.

The influence of TSI on the climate is multifaceted. Variations in TSI translate to different heating in various layers of the atmosphere (though UV here plays the major role), heat absorption in the oceans with different time scales from those of the atmosphere, differential heating over land and oceans, etc. These primary influences from TSI will in turn alter such things as atmospheric circulation, water vapour content in the atmosphere, and cloud cover. Effects from these secondary phenomena may then feed back into the energy absorbed by the climate system from solar irradiation, for example via changes in the Albedo, possibly enhancing the effects of TSI variations.

Due to the geographically heterogeneous nature of solar influence on climate and the rather complicated feedback mechanisms involved in solar forcing of the climate any simple explanation of TSI-climate connections is likely to fail, except in limited cases such as variations in sea surface temperature that seem to be at least partly explainable by simple energy balance considerations.

Satellite measurements of TSI started in November 1978 and have been continued since by various instruments. These instruments do not agree to better than 0.2% in the absolute value of TSI, but in relative changes of TSI they agree to better than 0.01%. Fröhlich and Lean, 1998, and Lee III et al., 1995, have constructed continuous time series of TSI from these satellite data from 1978 to the present, fluctuating around 1367 W/m^2.

Reconstructions of TSI based on proxy data, e.g., sunspot number, have been constructed going back through the Maunder minimum (Lean et al., 1995, Hoyt and Schatten, 1993, and others). These reconstructions agree qualitatively, though in absolute numbers there are significant differences. In fact, just going back 1-2 decades prior to the onset of satellite observations of TSI various reconstructions of TSI differ by as much as the variability within a solar cycle. This must be borne in mind when using reconstructed TSI for any climate correlation purpose.

Over a solar cycle TSI varies approximately 1.3 W/m^2 from solar min to solar max. With the geometric factor of ¼ and the Earth's Albedo of 0.7 this translates to a forcing of the atmosphere of 0.23 W/m^2. With a climate sensitivity of 0.6-0.8 $K/(W/m^2)$, (e.g., Appendix 9.1, Houghton et al., 2001), estimated from the average response of climate models to a doubling of CO2 this translates to a response of 0.14-0.18 K between solar max and solar min. However, the tropospheric temperature varies with approximately 0.5 K over a solar cycle. A direct forcing from TSI is therefore not sufficient to explain the variation of tropospheric temperatures and some amplification mechanisms would be required for TSI to be the main driver of the tropospheric temperature variability.

There are a large number of studies with the effects of changing TSI in general circulation models. Haigh (1999) gives a short introduction to some of these results. In general, the models all reproduce an increase in global average surface air temperature with increasing solar radiation, however they differ strongly in the geographical distribution of this warming, e.g., showing stronger responses in South America and the Arctic Ocean (Rind and Overpeck, 1993), mid- to high-latitudes (Nesme-Rimes et al., 1993), or northern hemisphere land areas (Cubasch et al., 1997). Haigh comments that the lack of a clear pattern between the models is an indicator "that the physical representations, in at least some of the models, are inadequate to the task."

GCMs are often applied in the detection and attribution of the component causes of climate change (see e.g. IPCC reports). In this technique the geographical *patterns* of response to particular forcing factors are pre-determined from the GCMs; it is assumed that the time-dependences of the forcing factors are known but that the *amplitudes* of the climate responses are unknown. The task is then essentially to perform a multiple regression analysis on a dataset to find which weighted combination of the response patterns best matches the data, taking into account known errors/uncertainties in both the data and patterns. Stott et al (2003), however, suggest that this method might have a bias against weak signals lost in the sampling noise. If that is the case these studies could underestimate the importance of natural factors and attributed a larger effect to anthropogenic causes of climate change. By running experiments in which natural forcings were enhanced Stott et al found that their model appears to be underestimating the solar influence by a factor of 2 or 3, while slightly overestimating the role of GHGs. The authors have some caveats and reservations about their results but note that the conclusion is supported by two other studies: Hill et al. (2001) find that models underestimate the solar response in tropospheric temperatures by a factor of 2 to 3, and North and Wu (2001) find an underestimate for near-surface temperatures of about 2.

6 Modelling

Global Climate Models (GCMs) are computer simulations of the state of the atmosphere-ocean system and its variability. They have become increasingly important as tools of the

climate scientist. Using numerical representations of processes involved, GCMs enable studies of complex interactions within the climate system, their evolution and sensitivity to internal or external forcing factors.

The atmosphere is a continuous, compressible fluid resting on the surface of a rotating planet. By applying some of the basic laws of physics - conservation of energy, conservation of mass, Newton's 2nd law of motion and the ideal gas law – to this fluid we can acquire an understanding of the main features of the global atmospheric circulation. Global Climate Models (GCMs) simulate the state and evolution of the atmosphere through solving the equations of motion at all points on a grid discretised in space and time. The starting point, considering first only dry air, is equations of continuity and momentum, the equation of state for the atmosphere, and the First Law of Thermodynamics. These provide 6 equations for 6 unknowns, the velocity u (three components), the pressure p, the density ρ, and the temperature T. Given initial and boundary conditions, some properties of dry air (M, C_p, η) and, importantly, a grid of values of the diabatic heating rate Q the equations can be solved in space and iterated in time to produce 4-dimensional fields of the variables. There are, however, a number of complications that make this procedure somewhat less simple than it may first appear:

1. The specification of Q depends on model state. This requires that the radiative transfer equation be solved as a function of the model fields of temperature and composition at each time-step.
2. The presence of water is fundamental to the state of the atmosphere providing sources/sinks of latent heat and clouds which have a huge impact on Q. Thus water vapour has to be transported within the model and a scheme to represent convection and condensation needs to be included.
3. The discretisation in space and time results in rounding errors and also, possibly, numerically unstable solutions.
4. Some representations need to be included for factors which occur on scales smaller than the grid size but nevertheless impact the large scale, for example surface orography and turbulence.
5. Constraints on computer resources (processing speed, memory, storage) place limitations on what is possible, requiring compromises to be made in grid resolution and/or the detailed representation of particular processes.

Radiative processes

In order to simulate the radiation budget, and to calculate the radiative component of the diabatic heating term, Q, it is necessary to invoke the radiative transfer equation. This gives the change in intensity of radiation of wavelength λ in direction between positions s and s+ds. Even to evaluate this one equation requires a large number of computations but to evaluate the diabatic source term, Q, in a GCM it is necessary to integrate the expression over all angles and wavelengths. Clearly it is not computationally feasible to incorporate in a GCM the full details of the expression and a range of approximations need to be made. Some of these are listed, along with the associated reduction in typical numbers of calculations, in Table 9. Each approximation brings a loss of accuracy and the choice of radiation scheme will be determined by a compromise between required accuracy and computational demands. The final row of the Table gives the Newtonian cooling approximation in which heating is assumed proportional to local temperature.

This is usually not sufficiently accurate (especially in the troposphere) and most GCMs adopt a band model approach. The number of spectral bands necessary also depends on the height regime of the model. For example, if it is intended to assess the effects of solar UV radiation in the middle atmosphere then extra shortwave bands need to be added to GCM radiation schemes which have been designed for use in the troposphere.

Approximation	Sum over spectral lines in expression for optical depth	Integration over height in expression for optical depth	Integration over height of irradiance contributions	Integration over zenith angle	Integration over wavelength	Total number of calculations	Number of exponentials in transmittance and Planck functions
None	1-10	10-100	10-100	1-10	10^4	$10^6 – 10^{10}$	10^5-10^6
Curtis-Godson	1-10	-	10-100	1-10	10^4	$10^5 – 10^8$	10^5-10^6
Diffusivity	1-10	-	10-100	-	10^4	$10^5 – 10^7$	10^5-10^6
Band model	-	-	10-100	-	1-10	$10 – 10^3$	$10 – 10^3$
Newtonian cooling	-	-	-	-	-	1	-

Table 9: Approximations in the radiative transfer equation (neglecting scattering) and the number of calculations needed for each component integral. Note that the total number is the product, not the sum, of the components because the integrals are nested. The final column gives the number of exponential functions that need to be estimated – each adding a further computational overhead.

Clouds

Clouds have a major impact on the heat and radiation budgets of the atmosphere. They transport latent heat from the oceans to the atmosphere. They reflect solar radiation back to space, reducing the net incoming radiative flux, and they trap infrared radiation, acting in a similar way to greenhouse gases. The magnitudes of these effects depend on the location, altitude, time of year and also the physical properties of the cloud.

Uncertainties and approximations in the representation of cloud formation and cloud radiative properties remain a major cause of uncertainty in current climate prediction models. Cloud formation depends on factors ranging from local topography, large scale flow and the temperature and humidity of air masses to the microphysical composition of particulates in the atmosphere. With grid sizes of the order of 100km in the horizontal and 1km in the vertical, there is no possibility of GCMs being able to reproduce realistic cloud structures down to convective scale so they include a variety of parameterizations for cloud prediction. On the largest spatial scales and annual timescales these parameterizations have limited success. For local cloud on timescales of hours, however, the predictions can be very poor. Even disregarding the problems associated with predicting cloud distributions the models still need to calculate the effects of the cloud on the radiation fields. Again gross approximations have to be made in terms of the microphysical properties of the water or ice particles and the method by which to carry out necessary integrations over spectral and spatial variables.

Discretization

The equations of motion cannot be solved analytically so numerical techniques need to be employed. Approximate solutions can be found using finite difference or series expansion methods in which the continuous functions of the variables are replaced by values on a finite number of spatial and/or temporal nodes (see e.g. Jacobson, 1999). The finite difference approach involves mapping the variables onto a grid and replacing the differential operator, ∂, by a discrete difference, Δ. There is no unique way of accomplishing this and the choice of approximation will depend on requirements with regard to accuracy, stability and convergence for the equation(s) in question.
Numerous schemes have been constructed using various combinations of approximations for the time and space differentials. Higher order approximations tend to be more stable but to smooth out fine structure in the fields. The stability of a scheme also depends on the grid-spacing; for example, the finite difference form of the advection equation tends to become unstable if the time step is greater than the ratio of the grid length to the maximum speed (i.e. the shortest time taken to cross a grid box).

Turbulence

At the surface of the Earth the air flow is necessarily zero but in a thin (50-300m) layer above the surface wind speeds increase logarithmically with height creating a shear layer. This wind shear produces eddies, on all scales up from the molecular, which result in the turbulent transfer of heat and momentum both horizontally and vertically. Surface obstacles such as rocks, trees, buildings also give rise to wind shear and turbulence while surface heating causes thermal turbulence and convection throughout the atmospheric boundary layer (extending up to between 0.5 and 3km). Clearly it is not possible for a model with a horizontal grid spacing of hundreds of kilometers and a vertical resolution of a few kilometers to simulate the details of these eddies but some representation needs to be included of their bulk effect on the momentum and heat budgets. This is usually done using a tensor **K** of eddy diffusion coefficients so, for example, the momentum equation will include an additional term where the eddy diffusion coefficients can be specified as functions of location and season or determined as a function of model state (e.g. wind shear, static stability). This approach is also sometimes used at the top of a model domain, not so as to represent any physical process but merely to ensure that high wind speeds do not develop near the upper boundary.

Models of reduced complexity

For climate simulations with GCMs it is often desirable to carry out an ensemble of runs, each with slightly different initial conditions, such that the spread in results provides an indication of intrinsic uncertainty. This imposes a significant overhead in terms of computing requirements. Computational demands also constrain possibilities with regard to the inclusion of what would be regarded as the best possible representation of all the known relevant physical and chemical processes. In practice, however, the latter may not be desirable – sometimes interpreting GCM output is almost as difficult as interpreting data from the real atmosphere. Under such circumstances it is often more useful to use simplified models which focus on one (or more) aspects of a problem at the expense of the treatment of other features which are deemed to be less important in the particular context.

A common approach is to reduce the dimensionality of the model, at the expense of a complete representation of dynamical processes. For example, 2D (latitude-height) models, in which zonal mean quantities are considered, have been successfully used in studies of stratospheric photochemistry and radiative transfer, including the response to solar variability (see e.g. Haigh, 1994). Although there is no overt longitudinal variability in 2D models, the diurnal variation in solar zenith angle is included in the photochemical and radiation schemes. 1D (height only) Energy Balance Models, which have no transport apart from vertical diffusion, can provide a useful first order estimate of global mean response to radiative forcing perturbations.
Alternatively, if the focus of attention is on a process occurring in a particular region of the atmosphere, it may be useful to restrict the spatial extent of the model, although care must then be taken with boundary conditions. Some interesting work on links between solar variability, the QBO and polar stratospheric temperatures has been carried out with a model in which the lower boundary was set at the tropopause, thus avoiding the necessity to simulate the complex cloud-radiation and boundary layer effects within the troposphere and allowing long integrations to take place (Gray et al, 2005).
Another approach is to simplify the treatment of certain processes in order to focus on others. For example, studies of coupling between the tropical lower stratosphere and tropospheric circulations, aimed at investigating potential solar amplification mechanisms, have been carried out by Haigh et al (2005) using a model in which all diabatic processes have been reduced to Newtonian relaxation to a reference equilibrium temperature. This maintains the full representation of dynamical processes but avoids the necessity for detailed calculations of Q thus allowing numerous experiments to be carried out.

Modelling studies of the solar modulation of climate via UV have traditionally been carried out by first estimating the predicted ozone changes between solar minimum and solar maximum (or 20th century versus Maunder Minimum values) using 2-D models that include relatively sophisticated chemical schemes. These monthly-averaged, zonally-averaged ozone changes are then used as input to the radiation schemes of full GCM simulations. In this way, the temperature and circulation response to the ozone changes can be assessed, although there is no possibility for those temperature and circulation changes to interactively feed back onto the ozone distributions. The prime methodology employed to assess the impact of including these additional ozone changes is to carry out model simulations with only TSI changes and compare them with simulations with both TSI and ozone changes. Most 'process' modelling studies, that seek to simulate the solar signal and thence explore the process mechanisms, employ models that extend from the ground to around 80 km in order to fully resolve the ozone distribution in the stratosphere. Most of the modelling studies are unable to reproduce the secondary temperature (and ozone) maximum in the lower stratosphere. This is important because it not only represents a deficiency in the simulation of the middle atmosphere itself but also means that the stratospheric anomaly required as forcing for any stratosphere-troposphere coupling mechanisms is not adequately provided. It suggests an underestimation of the modelled dynamical feedback through a modification of the meridional circulation and this requires further investigation. There are also many deficiencies in the model simulations of the interaction between the solar and QBO influences (Labitzke et al.

2002) and these may be related to the same dynamical problems. Very few of the models employed include an adequate gravity wave parameterization scheme and this may be one factor that requires improvement (Arnold and Robinson, 2003).

Because of computing resource constraints, GCM simulations of solar influence have usually consisted of two 20-30 year runs, under perpetual solar minimum conditions and perpetual solar maximum conditions respectively, and the difference between the two runs used as an estimate of the peak-to-peak solar signal. By running for many years in 'perpetual' mode like this, the statistical significance of the results is substantially improved. In order to gain the equivalent statistical significance from a single simulation in which the time-varying 11-year solar signal is imposed, the simulation would need to be many hundreds of years long. Employing a coupled ocean-atmosphere model in which the ocean temperatures can adjust to the imposed solar changes is inappropriate for integrations of this type employed for 11-year solar cycle studies, because the atmosphere is never actually in solar minimum or maximum for long enough for the ocean to adjust to any great extent. In this case, the models are used with observed or climatological-mean sea surface temperatures imposed at their lower boundaries. On the other hand, estimates of longer term solar changes, such as those between 20th century and Maunder Minimum values, are more appropriately carried out using a coupled model in which the ocean temperatures are able to respond and feedback onto the atmosphere component of the model.

Recently, improved computing capabilities have allowed the development of GCMs that include fully-coupled chemistry schemes so that improved feedback is possible not only from the ozone changes on to the temperature and circulation patterns but vice versa. However, the use of these fully-interactive chemistry GCMs for studies of the solar cycle influence is still at a relatively immature stage (e.g. Labitzke et al. 2002, Tourpali et al. 2003, Egorova et al. 2004, Haigh et al. 2004, Langematz et al. 2005, Schmidt et al. 2006) and runs with both coupled oceans and chemistry have yet to be carried out.

7 Conclusions and Recommendations

Through the ISAC study the team has reached a number of conclusions below we summarize the most important of these. It is then followed by recommendations. As this is an ESA funded study, one recommendation deserves to be highlighted: better, easier, more user-friendly access to existing data sets. The norm for US generated data sets are easy to access, easy to download, well organised. European data sets are lacking in this these respects. Too often the data are, when freely available, not organised with the end user in mind.

Conclusions

The Sun:

- Sunspot number catches only part of solar activity
- The Sun's magnetic field drives short term changes
- Use therefore magnetic data for Sun-Climate studies
- Solar output predictability is at most years ahead
- Due to the complexity and time-varying nature of the Sun solar-climate coupling must be expected to be very complex and probably changing with time

Correlations:

- The overall solar cycle dominates solar-climate correlations.
- Statistically robust signals of the impact of solar variability have been detected throughout the stratosphere and troposphere in temperature, wind and atmospheric circulation. These include, when the Sun is more active,:
    - a warming of the upper and lower stratosphere in low-to-middle latitudes
    - a strengthening of the winter stratospheric polar night jet
    - vertical bands of warming in the mid-latitude troposphere
    - a weakening and poleward expansion of the tropical Hadley cells and a poleward shift of the Ferrel cells
    - a more positive tendency of the North Atlantic Oscillation
    - the solar signal in stratospheric temperatures and in the tropospheric polar modes of variability is modulated by the phase of the quasi-biennial oscillation
- Direct heating by absorption of solar ultraviolet radiation can explain most of the temperature response in the upper stratosphere but not the signals in the lower stratosphere and troposphere.
- When removing the solar cycle the most robust tropospheric correlations are seen with UV and cosmic rays.
- UV and GCR show negative(positive) bands of correlations with low clouds at mid-to-high latitudes. These bands are strengthened by removal of the solar cycle.
- On the surface only rather weak correlations are observed. This is to some extent due to the short time span of the available parameters such as the NDVI (vegetation), snow and ice data.
- At solar min/max a zonally averaged temperatures under solar max/min conditions show a negative/positive correlation with UV in the troposphere and similar, but with opposite sign with GCR.

Mechanisms, Models and Methods

- Correlation studies inherently assume a linear response to changes in forcing parameters. Any non-linear behaviour of the climate system is bound to cause problems.
- There are serious discrepancies between the solar signal in stratospheric ozone derived from satellite measurements and that suggested by chemistry-climate models.
- Uncertainty in the ozone signal also implies uncertainty in the value of solar radiative forcing of the troposphere.
- Some of the ozone discrepancy may be related to inadequate treatment in the models of the effects of solar energetic particles but these are unlikely to explain the ozone minimum shown in the tropical middle stratosphere.
- Solar signals near the tropical stratopause can be transmitted to the polar and tropical lower stratosphere through mechanisms involving wave-mean flow interactions.
- Perturbations to the winter stratospheric polar vortex appear to propagate downwards into the troposphere although the mechanisms involved are not clear.

- Heating of the tropical lower stratosphere can influence the temperature, wind and circulation of the troposphere through dynamical coupling that appears to depend on perturbing the behaviour of synoptic-scale eddies.

Recommendations

Methods

- In future analyses of solar climate relations it would be fruitful to
    - use wavelet methods
    - use solar magnetic field data
- To understand solar activity use MHD and low-dimensional models.
- To analyse solar activity use multi-resolution analysis of all scales and extend time series through reconstructions by using indicators.
- Solar output quantities EM (SOHO, SDO), SEPs (ACE, Rhessi, Stereo) and SW (SOHO, Ulysses, ACE) would preferably be presented in synoptic maps.
- Coupled chemistry-climate modelling studies of the response of the middle atmosphere to variations in solar UV and energetic particles are needed to disentangle radiative, photochemical and dynamical influences on temperature, wind and composition
- Fully-coupled ocean-atmosphere-chemistry simulations are desirable but currently limited by computational demands.
- Coupled thermosphere-ionosphere-mesosphere-stratosphere modelling simulations to investigate atmospheric coupling processes.
- The use of simpler mechanistic models to identify and diagnose particular mechanisms operating.
- A better understanding of the role of clouds in the climate, particularly with respect to feedbacks between different solar-climate mechanisms, is needed in order to distinguish the solar signal in these mechanisms.

Observations

- Future observations of solar activity: carry out high resolution (Hinode, Solar Orbiter) and 3D real-time synoptic observations of the flow and magnetic field (SDO).
- Continued measurements of solar irradiance from satellites, along with robust inter-calibration of instruments, are essential for refining estimates of solar input to the Earth, its temporal variability and spectral composition
- Continued measurements of stratospheric ozone (and other minor constituents) from satellites, along with robust inter-calibration of instruments, are needed to advance understanding of the ozone response to the Sun.
- Combined aerosol and cloud observations particularly in the lower troposphere.

Data

- Through better understanding of the Sun construct robust reconstruction of TSI using indicators.

- Through continued observations and inter-calibration create a reliable and well-organised data set of clouds (type, distribution, properties).
- Through continued observations and inter-calibration create a reliable and well-organised data set of clouds (type, distribution, properties).
- Better, easier, more user-friendly access to existing data sets.

References

Arnold, N.F. and T.R. Robinson, 2003. Solar cycle modulation of the winter stratosphere: the role of atmospheric gravity waves. *Adv. Space. Sci*., **31**, 2121-2126.

Baldwin, M. P. and T. J. Dunkerton, Stratospheric harbingers of anomalous weather regimes, *Science*, *294*, 581-584, 2001.

Beer, J., Long-term indirect indices of solar variability, Space Science Reviews, 94, 53–66, 2000.

Black, R. X., B. A. McDaniel, 2004: Diagnostic case studies of the Northern Annular Mode. *J. Clim*. **17**, 3990-4004.

Boberg, F. and H. Lundstedt, Solar wind variations related to fluctuations of the North Atlantic Oscillation, *Geophysical Research Letters, 29*(15), 2002.

Castanheira, J. M., H. F. Graf, 2003: North Pacific-North Atlantic relationships under stratospheric control? *J. Geophys. Res*. **108**, Art. No. 4036.

Crooks, S.A. and L.J. Gray, 2004: Characterisation of the 11-year solar signal using a multiple regression analysis of the ERA-40 dataset. *J. Clim*. **18**, 996-1015.

Cubasch, U., R. Voss, G.C. Hegerl, J. Waszkewitz, and T.J. Crowley, Simulation of the influence of solar radiation variations on the global climate with an ocean-atmosphere general circulation model, *Clim. Dyn., 13*, 757-767, 1997.

Damon, P. E., and J. L. Jirikowic, The Sun as a low-frequency harmonic oscillator, Radiocarbon, 34(2), 199–205, 1992.

Dickinson, R. E., Solar Variability and the Lower Atmosphere, *Bulletin of the American Meteorological Society, 56*(12), 1240-1248, 1975.

Egorova, T., E. Rozanov, E. Manzini, M. Haberreiter, W. Schmutz, V. Zubov and T. Peter, Chemical and dynamical response to the 11-year variability of the solar irradiance simulated with a chemistry-climate model, Geophysical Research Letters, 31(6), 2004.

Ferek, R.J., T. Garrett, P.V. Hobbs, S. Strader, D. Johnson, J.P. Taylor, K. Nielsen, A.S. Ackerman, Y. Kogan, Q. Liu, B.A. Albrecht, and D. Babb. Drizzle suppression in ship tracks. J. Atmos. Sci. 57, 2707-2728, doi:10.1175/1520-0469(2000)057, 2000

Frick, P., D. Galyagin, D. V. Hoyt, E. Nesme-Ribes, K. H. Schatten, D. Sokoloff, and V. Zakharov, Wavelet analysis of solar activity recorded by sunspot groups, Astronomy & Astrophysics, 328, 670–681, 1997

Fröhlich, C. and J. Lean, The Sun's total irradiance: Cycles, trends and related climate change uncertainties since 1976, *Geophysical Research Letters, 25*(23), 4377-4380, 1998.

Gill, A.E., *Atmosphere-Ocean Dynamics*, Academic, San Diego, California, 1982.

Gillett N. P., B. D. Santer, and A. J. Weaver, *Nature, 432*, doi:10.1038/nature03209, 2004.

Gray, L J, J D Haigh and R G Harrison, 2005. Review of the influences of solar changes on the Earth's climate. Hadley Centre Technical Note 62, Met Office, Exeter

Gringel, W., J. M. Rosen and D. J. Hofmann, Electrical Structure from 0 to 30 Kilometers, in The Earth's Electrical Environment, pp. 166-182, National Academy Press, Washington,D.C., 1986.

Haigh J. D., The impact of solar variability on climate, *Science*, *272*, 981-984, 1996.

Haigh, J. D., 1999: A GCM study of climate change in response to the 11-year solar cycle. *Quart. J. Roy. Meteorol. Soc.* **125**, 871-892.

Haigh, J. D., Modelling the impact of solar variability on climate, *Journal of Atmospheric and Solar-Terrestrial Physics, 61*(1-2), 63-72, 1999.

Haigh, J. D., The effects of solar variability on the Earth's climate, *Philosophical Transactions of the Royal Society of London Series A-Mathematical Physical and Engineering Sciences, 361*(1802), 95-111, 2003.

Haigh, J. D., M. Blackburn and R. Day, 2005: The response of tropospheric circulation to perturbations in lower stratospheric temperature. *J. Clim.* **18**, 3672–3691.

Haigh, J. D. and H. K. Roscoe, Solar influences on polar modes of variability, *Meteorologische Zeitschrift*, *15*, 371-378, 2006.

Hartley, D. E., J. Villarin, R. X. Black, C. A. Davis, 1998: A new perspective on the dynamical link between the stratosphere and troposphere. *Nature* **391**, 471-474.

Herman, J. R. and R. A. Goldberg, Sun, weather, and climate, NASA, Washington DC, 1978.

Hill, D. C., M. R. Allen, N. P. Gillet, S. F. B. Tett, P. A. Stott, G. S. Jones, W. J. Ingram and J. F. B. Mitchell, Natural and Anthropogenic causes of recent climate change, in Detecting and Modelling Regional Climate Change, edited by M. B. India and D. L. Bonillo, pp. 275-290, Springer-Verlag, 2001.

Hoppel, W. A., R. V. Anderson and J. C. Willet, Atmospheric electricity in the planetary boundary layer, in The Earth's Electrical Environment, pp. 149-165, National Academy Press, Washington,D.C., 1986.

Houghton, J. T., Y. Ding, D. J. Griggs, M. Noguer, P. J. van der Linden and D. Xiaosu, Climate Change 2001: The Scientific Basis, p. -881, Cambridge University Press, 2001.

Hoyt, D. V. and K. H. Schatten, New Information on Solar-Activity, 1779-1818, from Herschel, William Unpublished Notebooks, *Astrophysical Journal, 384*(1), 361-384, 1992.

Hoyt, D. V. and Schatten, K. H., A discussion of plausible solar irradiance variations, 1700-1992. *Journal of Geophysical Research 98*, 18 895-18 906, 1993.

Hoyt, D.,V. and K.H. Schatten, The role of the sun in climate change, Oxford University Press, New York, 1997.

IPCC Intergovernmental Panel on Climate Change 4th Assessment Report, 2007.

Jacobson MZ 1999 Fundamentals of Atmospheric Modelling. CUP

Keckhut, P., C. Cagnazzo, M.-L. Chanin, C. Claud and A. Hauchecorne, 2004: The 11-year solar-cycle effects on temperature in the upper stratosphere and mesosphere. Part I: Assessment of observations. *J. Atmos. Sol. Terr. Phys.* **67**, 940-947.

Kodera, K., 2002: Solar cycle modulation of the North Atlantic Oscillation: Implication in the spatial structure of the NAO. *Geophys. Res. Lett*. **29**, Art. No. 1218.

Kuroda, Y., K. Kodera, 1998: Interannual variability in the troposphere and stratosphere of the southern hemisphere winter. *J. Geophys. Res*. **103**, 13787-13799.

Kulmala M., Kerminen V., Anttila T., Laaksonen A., and O'Dowd C., Organic aerosol formation via sulphate cluster activation, *Journal of Geophysical Research*, vol. 109, d04205, doi:10.1029/2003JD003961, 2004

Labitzke, K., 2004: On the signal of the 11-year sunspot cycle in the stratosphere over the Antarctic and its modulation by the Quasi-Biennial Oscillation (QBO). *Meteorol. Z.* **13**, 263-270.

Labitzke, K. and H. van Loon, Connection Between The Troposphere And Stratosphere On A Decadal Scale, *Tellus A 47*, 275-286, 1995.

Labitzke, K., H. van Loon, 1999: The stratosphere (Phenomena, History and Relevance). Springer Verlag Berlin Heidelberg New York, 179pp.

Langematz, U., J.L. Grenfell, K. Matthes, P. Mieth, M. Kunze, B. Steil, C. Bruhl, 2005. Chemical effects in 11-year solar cycle simulations with the Freie Universitat Berlin Climate Middle Atmosphere Model with inline chemistry (FUB-CMAM-CHEM) *Geophys. Res. Lett*., **32**, art. no. L13803.

Larkin, A., J. D. Haigh, and S. Djavidnia, The effect of solar UV irradiance variations on the Earth's atmosphere, *Space Science Reviews*, *94*, 199-214, 2000.

Lean, J., J. Beer, and R. Bradley, Reconstruction of solar irradiance since 1610: Implications for climate change, Geophysical Research Letters, 22(23), 3195–3198, 1995.

Lee III, R. B., M. A. Gibson, R. S. Wilson, and S. Thomas, Long-term total solar irradiance variability during sunspot cycle 22, *Journal of Geophysical Research, 100*(A2), 1667–1675, 1995.

Liszka, L., Cognitive information processing in space physics and astrophysics, Pachart Publishing House, Tucson, 2003.

Lovejoy, E.R., J. Curtius, and K.D. Froyd, Atmospheric ion-induced nucleation of sulfuric acid and water, *Journal Of Geophysical Research*, 109, D08204, doi:10.1029/2003JD004460, 2004.

Lundstedt, H., L. Liszka, and R. Lundin, Solar activity explored with new wavelet methods, Annales Geophysicae, 23, 1505–1511, 2005.

Lundstedt, H., L. Liszka, R. Lundin, and R. Muscheler, Long-term solar magnetic activity explored with wavelet methods, Annales Geophysicae, 24, 1–10, 2006.

McCracken, K. G., G. A. M. Dreschhoff, D. F. Smart, and M. A. Shea, Solar cosmic ray events for the period 1561–1994: 2. The Gleissberg periodicity, Journal of Geophysical Research, 106(A10), 21,599–21,609, 2001.

Marsh, N. and H. Svensmark, Cosmic rays, clouds, and climate, *Space Science Reviews, 94*(1-2), 215-230, 2000a.

Marsh, N. and H. Svensmark, Low cloud properties influenced by cosmic rays, *Physical Review Letters, 85*(23), 5004-5007, 2000b.

Marsh, N. and H. Svensmark, Galactic cosmic ray and El Nino Southern Oscillation trends in International Satellite Cloud Climatology Project D2 low-cloud properties, *Journal of Geophysical Research-Atmospheres, 108*(D6), 2003a.

Marsh, N. and H. Svensmark, Solar influence on Earth's climate, *Space Science Reviews, 107*(1-2), 317-325, 2003b.

Nesme-Rimes, E., E.N. Ferriera, R. Sadourny, H. LeTreut, and Z.X. Li, Solar dynamics and its impact on solar irradiance and the terrestrial climate, *J. Geophys. Res., 98,* 18923-18935, 1993.

North, G. R. and Q. G. Wu, Detecting climate signals using space-time EOFs, *Journal of Climate, 14*(8), 1839-1863, 2001.

Ogurtsov, M. G., Y. A. Nagovitsyn, G. E. Kocharov, and H. Jungner, Long-period cycles of the Sun's activity recorded in direct solar data and proxies, Solar Physics, 211, 371–394, 2002.

Peristykh, A. N., and P. E. Damon, Persistence of the Gleissberg 88-year solar cycle over the last 12,000 years: Evidence from cosmogenic isotopes, Journal of Geophysical Research, 108(A1), doi:10.1029/2002JA009390, 2003.

Randel, W. J., F. Wu, D. J. Gaffen, 2000: Interannual variability of the tropical tropopause derived from radiosonde data and NCEP reanalyses. *J. Geophys. Res.* **105**, 15509-15523.

Reames, D. V., Solar energetic particle variations, Advances in Space Research, 34, 381–390, 2004.

Reid, G. C., Influence of Solar Variability on Global Sea-Surface Temperatures, *Nature, 329*(6135), 142-143, 1987.

Reid, G. C., Solar Total Irradiance Variations and the Global Sea-Surface Temperature Record, *Journal of Geophysical Research-Atmospheres, 96*(D2), 2835-2844, 1991.

Reid, G. C., Solar variability and the Earth's climate: Introduction and overview, *Space Science Reviews, 94*(1-2), 1-11, 2000.

Rind, D. and J. Overpeck, Hypothesised causes of decade-to-century-scale climate variability: climate model results, *Quat. Sci. Rev*., 12, 357-374, 1993.

Sato, M., J. E. Hansen, M. P. Mccormick and J. B. Pollack, Stratospheric Aerosol Optical Depths, 1850-1990, *Journal of Geophysical Research-Atmospheres, 98*(D12), 22987-22994, 1993.

Schmidt, H., G. P. Brasseur, M. Charron, E. Manzini, M. A. Giorgetta, T. Diehl, V. I. Fomichev, D. Kinnison, D. Marsh, S. Walters, 2006. The HAMMONIA Chemistry Climate Model: Sensitivity of the Mesopause Region to the 11-Year Solar Cycle and CO2 Doubling. *J. Clim.*, **19**, 3903-3931.

Stott, P. A., G. S. Jones and J. F. B. Mitchell, Do models underestimate the solar contribution to recent climate change?, *Journal of Climate, 16*(24), 4079-4093, 2003.

Thejll, P., B. Christiansen, H. Gleisner, 2003: On correlations between the North Atlantic Oscillation, geopotential heights, and geomagnetic activity. *Geophys. Res. Lett*. **30**: Art. No. 1347.

Thompson, D. W. J., S Solomon, 2002: Interpretation of recent Southern Hemisphere climate change. *Science* **296**, 895-899.

Thompson, D. W. J., M. P. Baldwin, S Solomon, 2005: Stratosphere-troposphere coupling in the Southern Hemisphere. *J. Atmos. Sci.* **62**, 708-715.

Thompson, D. W. J.and S. Solomon, Recent stratospheric climate trends as evidenced in radiosonde data: Global structure and tropospheric linkages, *Journal of Climate, 18*,

Tourpali, K., C. J. E. Schuurmans, R. van Dorland, B. Steil and C. Bruhl, Stratospheric and tropospheric response to enhanced solar UV radiation: A model study, *Geophysical Research Letters, 30*(5), 2003.

Usoskin, I. G., N. Marsh, G. A. Kovaltsov, K. Mursula and O. G. Gladysheva, Latitudinal dependence of low cloud amount on cosmic ray induced ionization, *Geophysical Research Letters, 31*(16), 2004.

Usoskin, I. G., O. G. Gladysheva, and G. A. Kovaltsov, Cosmic ray-induced ionization of the atmosphere: spatial and temporal changes, *Journal of Atmospheric and Solar-Terrestrial Physics, 66,* 1791-1796, 2004.

van Loon, H., K. Labitzke, 1994: The 10-12 year atmospheric oscillation. *Meteorol. Z.* **3**, 259-278.

Viggiano, A. A. and F. Arnold, Ion Chemistry and Composition of the Atmosphere, in Handbook of Atmospheric Electrodynamics, edited by H. Volland, pp. 1-26, CRC Press, Washington,D.C., 1995.

Wagner, G., J. Beer, J. Masarik, R. Muscheler, P. W. Kubik, W. Mende, C. Laj, G. M. Raisbeck, and F. Yiou, Presence of the solar de Vries cycle (_205 years) during the last ice age, Geophysical Research Letters, 28(2), 303–306, doi:10.1029/2000GL006116, 2001.

White, W. B., J. Lean, D. R. Cayan and M. D. Dettinger, Response of global upper ocean temperature to changing solar irradiance, *Journal of Geophysical Research-Oceans, 102*(C2), 3255-3266, 1997.

Yu, F. Q., Altitude variations of cosmic ray induced production of aerosols: Implications for global cloudiness and climate, *Journal of Geophysical Research-Space Physics, 107*(A7), 2002b.

Yu, F., Binary H2SO4-H2O homogeneous nucleation rates based on a kinetic quasi-unary model: Look-up tables, *Journal of Geophysical Research,* doi:10.1029/2005JD006358, in press. 2006

Yu, F., and R. P. Turco, Ultrafine aerosol formation via ion-mediated nucleation, *Geophysical Research Letters*, 27, 883. 2000